European Journal of Medicinal Chemistry 250 (2023) 115177

Contents lists available at ScienceDirect

European Journal of Medicinal Chemistry

journal homepage: www.elsevier.com/locate/ejmech

Research paper

Tuning liver pyruvate kinase activity up or down with a new class of allosteric modulators

Amalyn Nain-Perez [a], Oscar Nilsson [a], Aleksei Lulla [c], Liliana Håversen [b], Paul Brear [c], Sara Liljenberg [a], Marko Hyvönen [c], Jan Borén [b], Morten Grøtli [a,*]

[a] Department of Chemistry and Molecular Biology, University of Gothenburg, SE-412 96, Gothenburg, Sweden
[b] Department of Molecular and Clinical Medicine, University of Gothenburg and Sahlgrenska University Hospital, SE-413 45, Gothenburg, Sweden
[c] Department of Biochemistry, University of Cambridge, Cambridge, CB2 1GA, United Kingdom

ARTICLE INFO

Keywords:
Pyruvate kinase
PKL
Modulation
Enzyme activity
Activation
Inhibition

ABSTRACT

The liver isoform of pyruvate kinase (PKL) has gained interest due to its potential capacity to regulate fatty acid synthesis involved in the progression of non-alcoholic fatty liver disease (NAFLD). Here we describe a novel series of PKL modulators that can either activate or inhibit the enzyme allosterically, from a cryptic site at the interface of two protomers in the tetrameric enzyme. Starting from urolithin D, we designed and synthesised 42 new compounds. The effect of these compounds on PKL enzymatic activity was assessed after incubation with cell lysates obtained from a liver cell line. Pronounced activation of PKL activity, up to 3.8-fold, was observed for several compounds at 10 μM, while other compounds were prominent PKL inhibitors reducing its activity to 81% at best. A structure-activity relationship identified linear-shaped sulfone-sulfonamides as activators and non-linear compounds as inhibitors. Crystal structures revealed the conformations of these modulators, which were used as a reference for designing new modulators.

1. Introduction

Glucose metabolism in human cells depends on the glycolytic enzyme pyruvate kinase (PK), which is part of a cytoplasmic metabolic pathway [1,2]. PK catalyses the last and irreversible step of the glycolysis, where the phosphoryl group of phosphoenolpyruvate (PEP) is transferred to adenosine diphosphate (ADP) to produce adenosine triphosphate (ATP) and pyruvate [3]. The product pyruvate participates in various metabolic processes, and thus PK is considered crucial not only for the glycolytic pathway but also for the entire cellular metabolism [4]. In vertebrates, four different PK isoforms have been identified [5], encoded by two genes (PKM and PKLR). Alternative splicing of the PKM transcript generates isoforms PKM1 and PKM2, while another splicing of the PKLR transcript generates PKL and PKR [3]. Type M1 is the major isozyme of cardiac muscles and the brain and is the only isozyme found in adult skeletal muscles. Type M2 is widely distributed throughout the body and is the minor isozyme found in the liver and commonly derived from kidneys and leukocytes. The L type is the major isozyme in the liver, and the R type is mainly found in erythrocytes [3,5,6]. The mammalian PK isoenzymes R, L, and M2, are naturally activated by PEP and fructose-1,6-bisphosphate (FBP) [5].

More recently, PKL has attracted additional attention due to its identification as a candidate gene for regulating fatty acid synthesis and oxidation involved in the progression of non-alcoholic fatty liver disease (NAFLD) [7–9]. NAFLD is a collection of hepatic conditions in which excess fat accumulates in the liver [10,11]. NAFLD is the most prevalent liver condition worldwide and is closely associated with the onset of obesity and type 2 diabetes [11]. In addition, prolonged NAFLD puts affected individuals at increased risk of developing more severe conditions such as hepatic steatohepatitis, liver cirrhosis and hepatocellular carcinoma [11]. Although NAFLD is the most common cause of chronic liver disease in developed countries, and its worldwide prevalence continues to increase along with the growing obesity epidemic, there is no approved pharmacological treatment for NAFLD.

In previous work, we identified small molecules capable of modulating PKL by using ADP-competitive inhibitors as a target for drug discovery for NAFLD [12]. The complications with targeting the active site of PKs include the highly charged nature of the active site and the need to compete with natural ligands. However, using an allosteric site to modulate the target could overcome the issue of competition with

* Corresponding author.
E-mail address: grotli@chem.gu.se (M. Grøtli).

https://doi.org/10.1016/j.ejmech.2023.115177
Received 30 December 2022; Received in revised form 30 January 2023; Accepted 31 January 2023
Available online 1 February 2023

natural ligands. Allosteric modulators can potentially increase or decrease the enzyme's catalytic activity while still allowing the natural ligand to bind to the active site [13]. Multiple allosteric sites have been identified in PK isoforms, both natural binding ligands such as FBP and synthetic ligands [4,14]. Several allosteric activators have been reported for PKM2 [15–20]. Along with mitapivat, a PKR activator approved for treating adults with pyruvate kinase deficiency [21]; it can bind at the interface of two protomers in tetrameric forms of PKR, different from the allosteric site of FBP on the tetramer form [22]. We assumed a similar binding pocket would be present in the PKL tetramer.

In this paper, we explore the allosteric site, which is found at the interface formed between the A domains of adjacent protomers of PKL. We describe the discovery of a class of allosteric modulators that fall into two categories that are capable of either activating or inhibiting the activity of PKL. Starting from polyphenolic metabolite urolithin D, which has attracted attention as a potential agent for the prevention and treatment of liver disease [23]. We first deconstructed the original inhibitor and then designed a series of hybrid compounds by combining crystal structure analysis of PKL-ligand complexes and *in vitro* screening. These compounds represent an exciting new class of molecules to study the mechanism of allosteric regulation in PK and will guide the future development of PKL inhibitors.

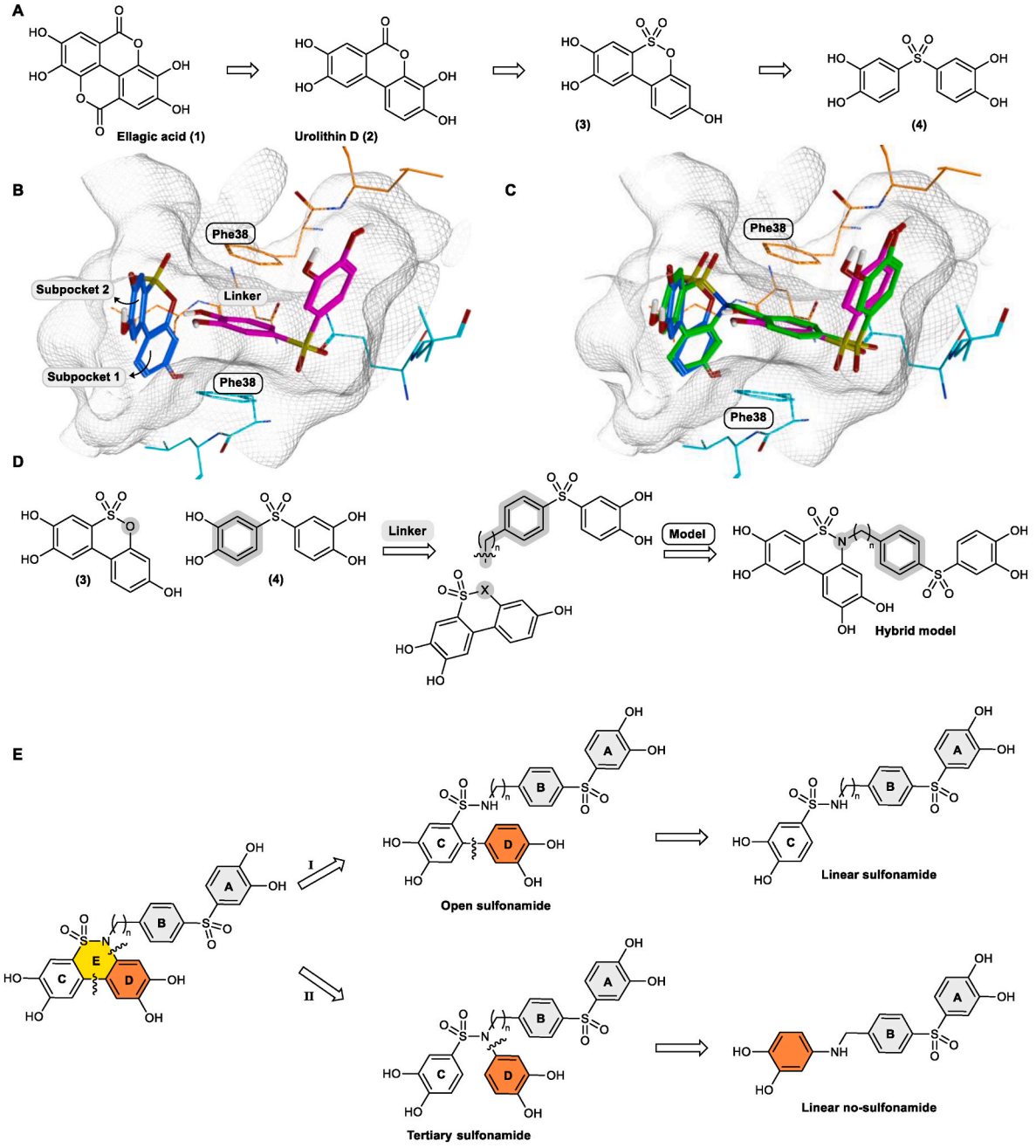

Fig. 1. Structural basis for the design of hybrid modulators of PKL. **A**) Structural representation of ellagic acid (**1**), urolithin D (**2**), and their synthetic derivatives **3** and **4**. **B**) Superposition of the crystal structures of **3** (blue carbons; PDB: 7FRW) and **4** (magenta carbons; PDB: 7FRV) in the allosteric site. **C**) Modelled hybrid compound (green carbons) designed using a superposition of both crystal structures **3** and **4** in the cavity of the allosteric site. **D**) Proposed hybrid model based on fragments **3** and **4** with a benzylamine moiety used as the linker. **E**) Design of a hybrid sultam using a benzylamine ($n = 1$) or phenylethanamine ($n = 2$) as a linker. Multiple modifications afforded branched sulfonamides and linear sulfonamides.

2. Results and discussion

2.1. Design of the hybrid model

We have identified ellagic acid (**1**) and its natural metabolite, urolithin D (**2**), as allosteric PKL inhibitors, with 21% and 37% inhibition in liver cell lysate at 10 μM, respectively [24]. Several synthetic modifications of these natural products provided a series of sulfone-catechol-containing compounds as potent inhibitors of PKL (Fig. 1A).

Crystal structures were determined for tetrameric PKL soaked with two Urolihin D derivatives: A sulfone-containing **3** and a variant in which the central ring has been opened **4**. Analysis of these protein-ligand complexes shows how two molecules of **3** bind to the two large, symmetrical pockets on either side of the two phenylalanine residues (Phe38) from adjacent PLK molecules. The structure of **4**, a urolithin D derivative in which the central ring is opened, revealed an entirely different binding mode in this site, with one of the catechol rings sandwiched between the side chains of the Phe38 residues and the other catechol bound to the pocket where **4** binds. As the binding site is symmetrical across the dimer interface, two alternative molecules were found that could occupy both pockets. Compound **3**, with its three fused rings, fills the pocket fully, while **4** occupies only part of the pocket. Here we will call the site where only **3** binds to as subpocket 1 and the other side where the second half of **3** binds as subpocket 2. We refer to the space between the Phe38 side chains as the linker site (Fig. 1B).

Superposition of the crystal structures of two ligands in the allosteric site, **3** (PDB: 7FRW) and **4** (PDB: 7FRV), reveals a direct way to link the two molecules through the central ring of **4** and the catechol ring of **3** in the linker area (Fig. 1B). Guided by the crystal structures, we model a hybrid molecule in the allosteric site, where the sulfone group of **3** is replaced with a sultam group, creating a bond to connect it with **4** (Fig. 1C). One of the catechol groups of **4** was replaced with a benzyl group, to provide a linker between the two fragments (Fig. 1D). The linker's length (illustrated by the letter n) may be modified since the space in the area allows it. This variation may identify how linker size influences the interaction of the sulfone group with Phe38. Two approaches to the design of hybrid sultams are proposed (route I and route II, Fig. 1E).

We designed key intermediates to synthesise the hybrid model,

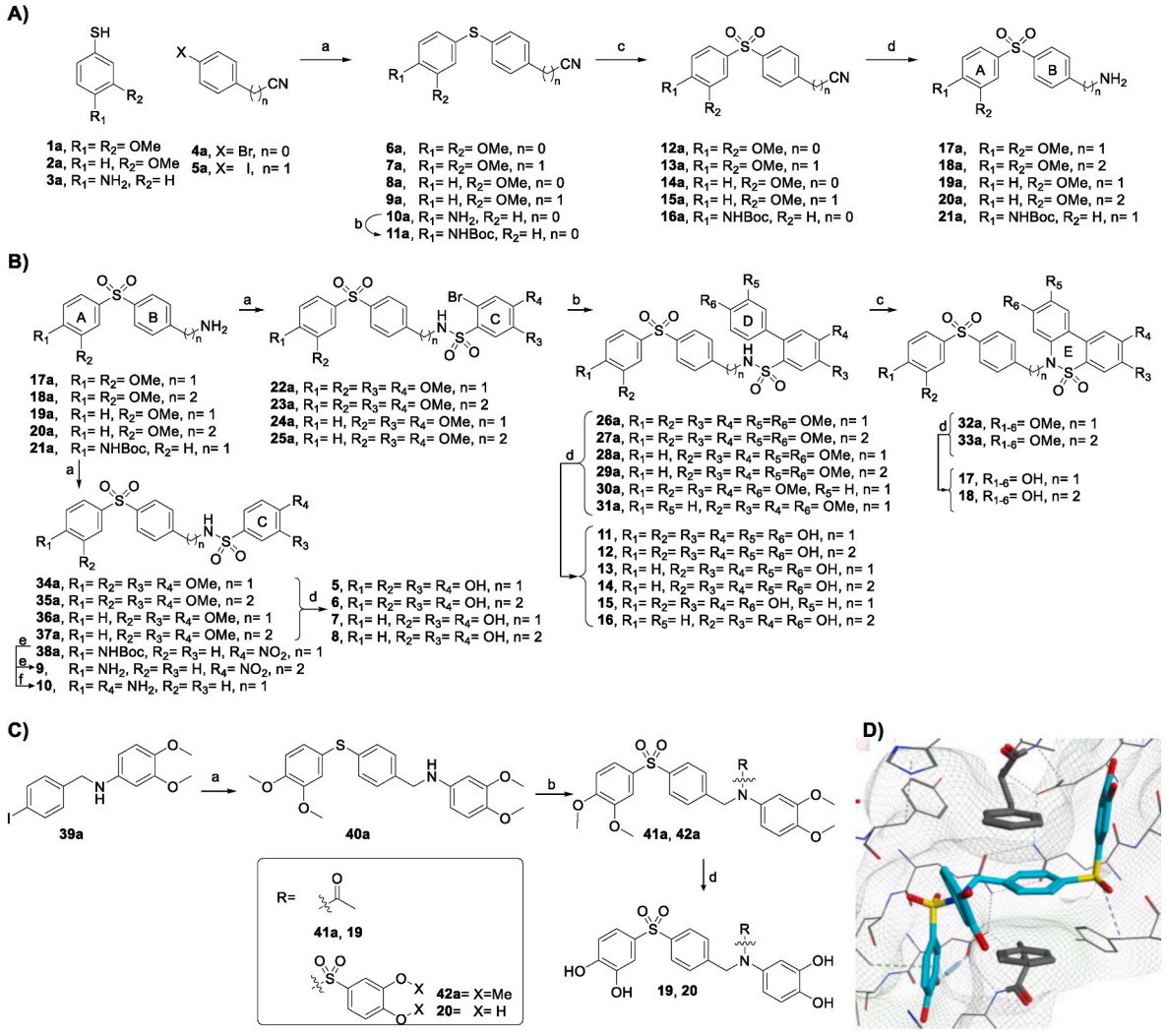

Scheme 1. Synthesis of first-generation hybrid compounds. *Reagents and conditions*. **A**) a) $Pd_2(dba)_3$, DPPF, DIPEA, toluene, 120 °C, 2–18 h, 81–98%; b) Boc. anh., H_2O, 130 °C, 1 h, MW, 97%; c) *m*CPBA, $CHCl_3$, 0 °C to r.t, 2 h, 81–99%; d) Pd/C, H_2, MeOH/DCM, HCl, r.t, 2–18 h, 52–92%. **B**) a) Ar-$SOCl_2$, DIPEA, DMF, r.t, 1 h, 55%–97%; b) $Pd(PPh_3)_4$, Ar–$B(OH)_2$, K_2CO_3, tol:EtOH:H_2O, 120 °C, 1 h, 47%–83%; ***c***) PIDA, I_2, K_2CO_3, DCM, 35 °C, 30 min, 32%–46%; d) BBr_3, DCM, 0 °C to r.t, 2 h, 22%–84%; e) DCM, r.t, CF_3COOH, 30 min, 61%; f) *i*) Fe, NH_4Cl, EtOH, THF, 60 °C, 6 h, *ii*) DCM, r.t, CF_3COOH, 1 h, 36%. **C**) For **39a**: 3,4-dimethoxyaniline and 1-(bromomethyl)-4-iodobenzene, MeCN, K_2CO_3, 120 °C, MW, 1 h, 50%; a) 3,4-dimethoxybenzenethiol, DIPEA, DPPF, $Pd_2(dba)_3$, toluene, 120 °C, 16 h, 98%; b) *i*) for **41a**: AcCl, DIPEA, DCM, 0 °C to r.t, 30 min, 91%; for **42a**: $ArSO_2Cl$, DIPEA, DCM, r.t, 23 h, 85%; *ii*) *m*CPBA, $CHCl_3$, r.t, 30 min, 96%; d) BBr_3, DCM, 0 °C to r.t, 2 h, 59%–73%. **D**) X-ray structure of **20** in complex with PKL (PDB: 7FS7).

which will be used to build the structure-activity relationship for this series. To construct such compounds, our first question was: Is the cyclic sultam required to generate an effect on the PKL activity? To address this, we designed an open sulfonamide (Fig. 1E, route I). The second question involved ring D of the open sulfonamide. How does the presence of ring D influence the biological activity of PKL? To answer this, we designed a so-called linear sulfonamide. Since the model suggested that the ring D filled subpocket 2, we questioned whether subpocket 2 could be filled by substituting sulfonamide, as proposed in the tertiary sulfonamide model, or if this is only required in the case of a link through ring C (Fig. 1F, route II). To compare the effect of the linear sulfonamide model, we also designed a model where an amine bond replaced the sulfonamide to explore the impact of this variation on the PKL activity.

In route (I), the synthesis started with the formation of the substructure containing rings A and B (Scheme 1A). The thioether intermediates (**6a**–**11a**) were prepared from commercially available thiols (**1a**–**3a**) and halogenated-aryl compounds (**4a**–**5a**) via a palladium-mediated coupling reaction. Subsequently, quantitative oxidation of the thioethers to the corresponding sulfone derivatives was carried out with *m*CPBA. Finally, the nitrile group was reduced via hydrogenation to yield the desired A/B ring system (**17a**–**21a**).

The linear compounds were formed using 3,4-dimethoxybenzenesulfonyl chloride or 4-nitrobenzenesulfonyl chloride when required (**34a**–**38a**), and the demethylation of these intermediaries yielded compounds **5**–**8**. Compound **38a** was treated with CF_3COOH to afford compound **9** and was separately treated with iron to give compound **10** (Scheme 1B).

To introduce ring D, compounds **17a**–**21a** were first reacted with sulfonyl chlorides containing ring C with a Br substituent in the *ortho* position, resulting in intermediaries (**22a**–**25a**), followed by a Suzuki coupling reaction to furnish compounds **26a**–**31a** (Scheme 1B). Deprotection of the methoxy groups by treatment with BBr_3 afforded compounds **11**–**16**. Intermediates **26a**–**31a** were treated with PIDA to generate the corresponding sultam derivatives (**32a**–**33a**), which, after demethylation yielded compounds **17**–**18**.

A

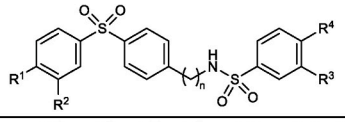

Compound	n	R^1	R^2	R^3	R^4	PKL activity (% Vehicle)$^{\alpha}$
5	1	OH	OH	OH	OH	143.6±10.6****
6	2	OH	OH	OH	OH	237.2±8.1****
7	1	H	OH	OH	OH	171±0.6**
8	2	H	OH	OH	OH	221.8±5.9****
9	1	NO_2	H	H	NH_2	no effect
10	1	NH_2	H	H	NH_2	203.1±10.4**

B

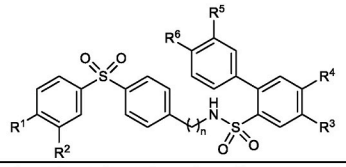

Compound	n	R^1	R^2	R^3	R^4	R^5	R^6	PKL activity (% Vehicle)$^{\alpha}$
11	1	OH	OH	OH	OH	OH	OH	48.6±1.7****
12	2	OH	OH	OH	OH	OH	OH	46.6±1.8****
13	1	H	OH	OH	OH	OH	OH	no effect
14	2	H	OH	OH	OH	OH	OH	121.5±15.4**
15	1	OH	OH	OH	OH	H	OH	32.2±2.7***
16	1	H	OH	OH	OH	H	OH	14.1±8.1*

C

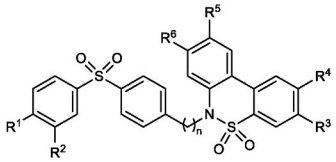

Compound	n	R^1	R^2	R^3	R^4	R^5	R^6	PKL activity (% Vehicle)$^{\alpha}$
17	1	OH	OH	OH	OH	OH	OH	47.1±1.6****
18	2	OH	OH	OH	OH	OH	OH	120.6±22*

D

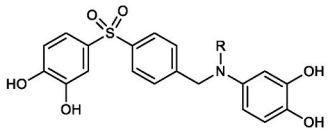

Compound	R	PKL activity (% Vehicle)$^{\alpha}$
19	Acetyl	38.7±3.6***
20	3,4-hydroxy-benzenesulfonyl	53.8±0.3****

E

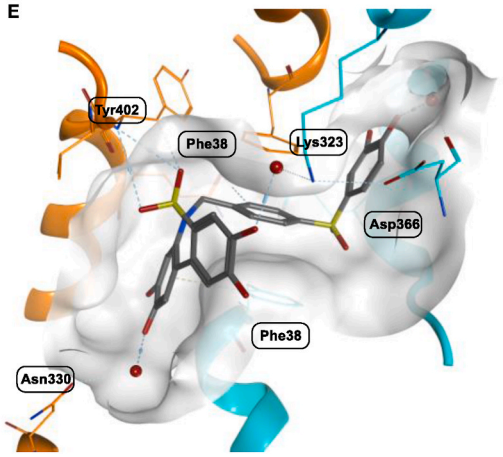

F

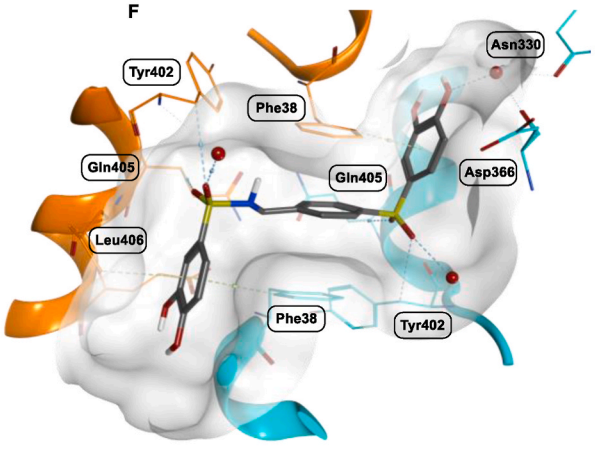

Fig. 2. Effects of compounds 5–20 on PKL activity and X-ray crystal structures of 5 and 17. **A**, **B**, **C**, **D**) Effects of hybrid combinations (**5–20**) on PKL activity in cell lysate. Mean ± SD, n = 3, *p < 0.05, **p < 0.01, ***p < 0.001, ****p < 0.0001, One Way ANOVA followed by Dunnett's multiple comparison test. $^{\alpha}$The compounds (10 μM) were incubated for 5 min at RT with cell lysates obtained from the HepG2 PKM2 KO liver cell line. The control cell lysates received a vehicle (DMSO) instead. The PKL activities of the cell lysates treated with the compounds were expressed as % of the PKL activity in the vehicle. **E**, **F**) Compounds **5** and **17** bound to the allosteric interface, the crystal structure of **5** bound to PKL (PDB: 7FRX), the crystal structure of **17** bound to PKL (PDB: 7FS5).

For route (II), from commercially available 3,4-dimethoxyaniline and 1-(bromomethyl)-4-iodobenzene, a nucleophilic substitution reaction gave compound **39a** (Scheme 1C), which was coupled to 3,4-dimethoxybenzenethiol through palladium catalysis to yield the thioether **40a**. Compound **40a** was used as a common intermediary to synthesise the linear compound **19**, and branched derivative **20**. Oxidation of thioether **40a** to the corresponding sulfone was challenging because of oxidation of the free NH-group. *N*-Boc protection was implemented; however, after the deprotection step, the compound appeared to be unstable. Next, the nitrogen was acetylated (**41a**), which, after the deprotection of the methoxy groups, afforded **19**. Compound **40a** was coupled with 3,4-dimethoxybenzenesulfonyl chloride followed by oxidation of the thioether with *m*CPBA to the yield the corresponding sulfone **42a**. Finally, treatment with BBr_3 gave compound **20**.

2.2. Unexpected effects of compounds 5–20 on PKL activity

To assess the effects of compounds **5**–**20** on PKL enzymatic activity, we incubated the compounds (10 μM) with cell lysates obtained from a liver cell line HepG2 from which PKM2 isoform has been knocked out and thus containing only the PKL isoform. The results are presented in Fig. 2A–D. The hybrid sulfonamides **11**, **12**, **15** and **16** and sultam **17** demonstrated weak inhibitory effects on the activity of PKL (14%–48% inhibition), except for **13**, **14** and **18**, which appeared inactive in the assay.

Additionally, a comparison between cyclic sultam **17** and open sulfonamide **11** indicates that open and cyclic sulfonamides have similar weak inhibitory effects on PKL activity. Surprising and unexpected results were observed for the impact of linear sulfonamides (**5–10**) on PKL activity. These compounds behave as activators of PKL, with increases in PKL activity ranging between 143% and 237%. Compounds **9** and **10** differ in the *p*-substitution of ring C, suggesting that an electron-donating group or H-bond is required at that position to preserve the activity. In contrast, compounds **19** and **20** showed that substitution of the NH-group inhibited the activity of PKL by 38% and 53%, respectively.

2.3. Activation and inhibition of hybrid compounds by binding conformation in the allosteric site of PKL

The X-ray crystal structure of **17** in complex with PKL (Fig. 2E, PDB: 7FS5) correlated well with the computational model. The linker forms π–π interactions with both Phe38 side chains, and the terminal groups sit in the expected conformations in the two pockets. The catechol of ring A occupies subpocket 1 (Fig. 2E) and interacts indirectly with Asp366 via a water molecule. One oxygen of the sulfone attaches to this catechol and interacts with the side chain of Gln405 (3.51 Å). Ring C binds to subpocket 1 of chain A, and the catechol interacts with Asp366 and Asn 330 through a water molecule. Ring C is also involved in a T-shaped π-interaction with one of the Phe38 side chains, while the catechol of ring D interacts with Lys323 through a bridging water molecule. Both oxygens of the sulfonamide group interact with Tyr402 (3.27 Å and 3.67 Å).

Similarly, compound **5** (Fig. 2F) shows ring A bound in subpocket 1, with chain C involved in a T-shaped π-interaction with Phe38A and the catechol group indirectly interacting with Asn330C and Asp366C through a water molecule. The oxygen of the sulfone group interacts with the side chains Gln405 and Tyr402 (3.60 Å and 3.69 Å, respectively). Ring B forms a π- π interaction with Phe38. The two oxygens of the sulfonamide form a side chain interaction with Gln405 and Tyr402 (3.37 Å and 3.51 Å, respectively), like sulfone on the other side. Ring C binds to subpocket 1 of chain A and is stabilised by a C–H π-interaction with Leu 406 and a T-shaped π-interaction with Phe38. Minor differences were observed between both X-ray structures; however, the electron density distribution of **5** is symmetrical, while the density distribution of **17** is more localised to the side on which both subpockets 1 and 2 are occupied (similarly is observed for compound **20**, Scheme 1D).

2.4. Proof of concept: switching activators to inhibitors

A series of diarylsulfonamides was reported in 2010 as potent activators of isoform M2 (Fig. 3A) [25]. Due to the similarities in the conformations of these compounds in the allosteric binding site with our reported series of activators (5–10), we used the diarylsulfonamide fragment of DASA-55 as a scaffold to synthesise two series of derivatives (Fig. 3A). A superposition of the ligand DASA-55 and 17 in the PKL crystal structure shows similarities in the sulfone-occupied site (Fig. 3B). This also shows that an extra ring D can be added to the DASA-55 scaffold. Thus, we generated a model based on our hypothesis (Fig. 3C) that the linear shape of these compounds activates the enzyme activity, and the introduction of ring D would inhibit PKL activity. To test this, we designed a small series of compounds containing a disulfonylpiperazine moiety (Fig. 3D) and analysed their effect on PKL activity in HepG2 KO PKM2 cell lysates (Fig. 3E).

Two different series of compounds were prepared from commercially available Boc-piperazine (Scheme 2). First, intermediary **43a** was prepared as a building block of Suzuki coupling with different boronic acids to afford (**44a**–**45a**). Subsequently, these intermediaries were coupled with nitro group-substituted sulfonyl chlorides (**46a**–**48a**). These were reduced into the corresponding anilines using iron, and following deprotection of the methoxy group by treatment with BBr_3 gave products **23**–**25**. The second series was achieved by treatment of the intermediate **49a** with the respective sulfonyl chloride to yield **50a**–**51a**, which underwent reduction of the nitro group followed by the deprotection of the methoxy groups (**21**–**22**).

2.5. Modulators that can either activate or inhibit PKL

As expected, the linear compounds **21** and **22** behave as activators (280%–380%), while compounds **23**–**25**, containing ring D, are inhibitors (44%–53%). We determined AC_{50} for the most active activator **21** using purified PKL enzyme in ATP-Glo assay as 1.39 μM (Fig. 3F). The structural difference between the series of activators and inhibitors is the presence of ring D, suggesting that the occupancy of subpocket 2 is related to the inhibition of PKL activity. The X-ray crystal structures of compounds **21** and **24** bound to PKL were determined, and as expected, both bind between Phe38 through a piperazine linker (Fig. 3G and H). A significant difference between **21** and **24** is the interaction formed by the catechol of ring D in **21** to Asp366 and Lys323 through water bridges.

2.6. The second generation of hybrid molecules: structure-activity relationship analysis

Since the allosteric site of this interface is composed of two protomers of PKL oligomer, the first generation of hybrid derivatives contained an aromatic ring in one of the two pockets. Here, we designed a second generation of hybrid derivatives as potential inhibitors. Our strategy consisted of the superposition of the crystal structure of **17** with the crystal structure of **4**, another class of inhibitor compound with similar characteristics, including bearing a catechol in subpocket 2 (Fig. 4A). Then, a new series of compounds was proposed (Fig. 4B and C) by presuming that a smaller molecule containing the substituents to fill subpockets 1 and 2 in one protomer would provide both occupancy of each pocket and perhaps an improved ability to reach the allosteric site.

A simple synthetic strategy was utilised to build several derivatives of the second-generation hybrids, as detailed in Scheme 3. Starting with commercially available 3,4-dimethoxybenzenesulfonyl chloride **52a**, substitutions with various commercially available anilines (**54a**–**57a**) afforded intermediaries (**58a**–**61a**). Additionally, to explore the effect of the substitutions on the nitrogen group of the sulfonamide, alkyl chains of different sizes were introduced via treatment with different alkyl

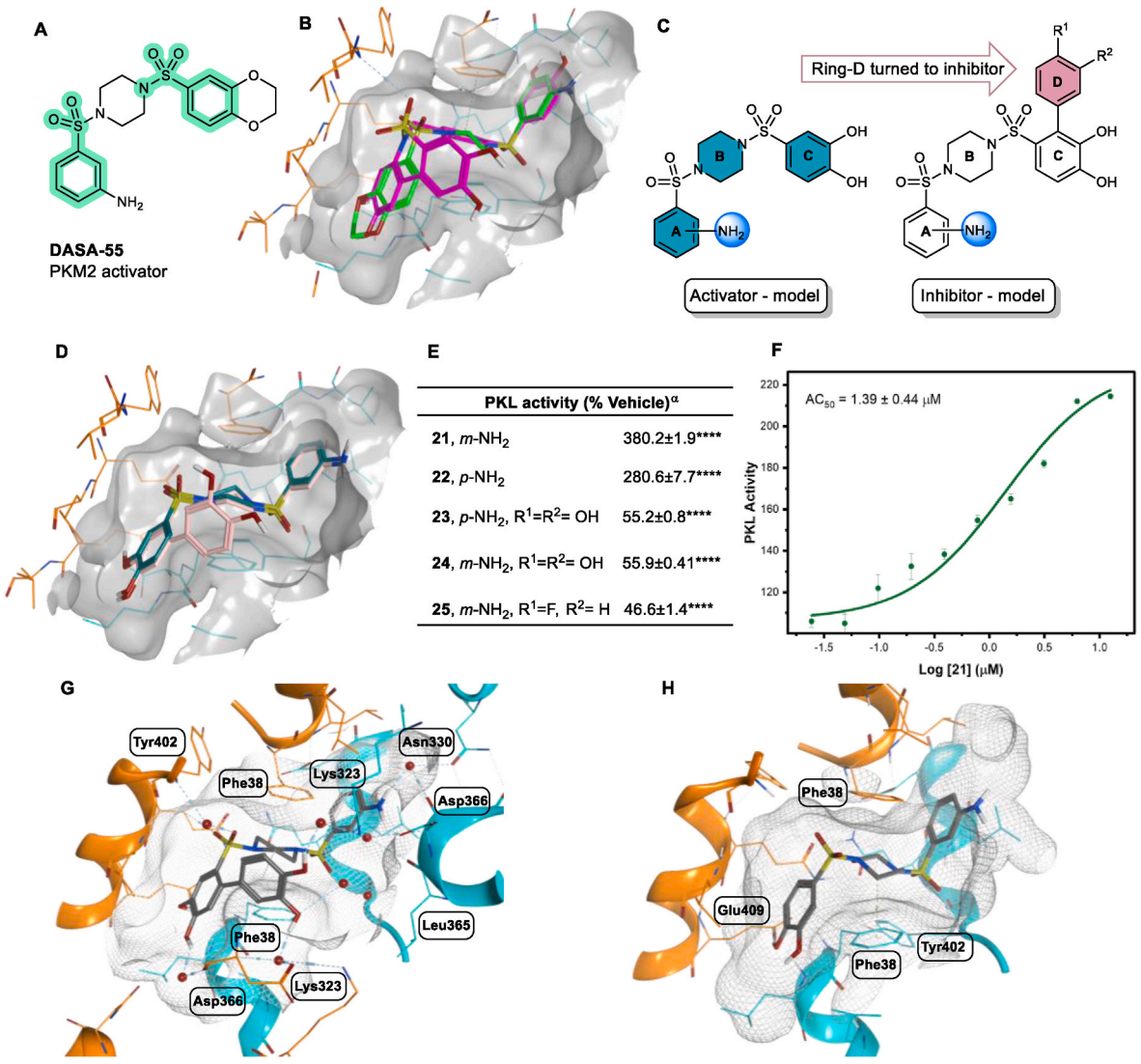

Fig. 3. Design for switching activators to inhibitors. **A**) Reported activator of PK isoform M2 containing a diarylsulfonamide scaffold. **B**) Overlapping molecular model of **DASA-55** (green carbons) in the allosteric site of PKL in complex with **17** (fuchsia carbons; PDB: 5SMQ). **C**, **D**) The proposed molecules as modulators (activators or inhibitors) of PKL are represented in 2D and 3D in the allosteric site of PKL. **E**) Effect of compounds **21**–**25** on PKL activity in HepG2 KO PKM2 cell lysates. Mean ± SD, n = 3, *p < 0.05, **p < 0.01, ***p < 0.001, ****p < 0.0001, One Way ANOVA followed by Dunnett's multiple comparison test. The PKL activities of the cell lysates treated with the compounds were expressed as % of the PKL activity in the vehicle (DMSO). **F**) AC_{50} curve for compound **21**, mean ± SD, n = 3. **G, H**) Diarylsulfonamide as an activator and inhibitor bound to PKL in the allosteric site; binding site of compound **24** (PDB: 7FSA) and compound **21** (PDB: 7FS8). [α]The compounds (10 μM) were incubated for 5 min at RT with cell lysates obtained from the HepG2 PKM2 KO liver cell line.

iodides/bromides, which afforded derivatives (**62a**–**67a**).

Subsequently, deprotection of the methoxy groups by treatment with BBr_3 yielded compounds **26**–**34**.6-Bromo-3,4-dimethoxybenzenesulfonyl chloride (**53a**) was used to prepare intermediates **68a–69a**. A Suzuki coupling reaction using (3,4-dimethoxyphenyl) boronic acid provided the aryl-aryl intermediaries (**70a**–**71a**). Methylation of **70a** was achieved by treatment with iodomethane to form compound **72a**. This series of compounds reacted quantitatively with BBr_3, affording deprotected hydroxy groups (**35**–**37**). In addition, a dimer version of **35** (**38**) was synthesised with the intent of the two catechol-bearing rings to fill both sub-pockets 2 symmetrically. Sulfonyl chloride (**53a**) was treated with the linker *N*,*N*-dimethylethane-1,2-diamine to provide the dimer **73a**, followed by palladium catalysis to generate the aryl–aryl coupling product **74a**. Final treatment with BBr_3 yielded **38**.

2.7. Tuning inhibitors of PKL

Cell lysate assays were used to evaluate the inhibitory effects of the new series of compounds **26**–**38** against PKL in HepG2 PKM2 KO cell lysates (Fig. 4D, H). Compounds containing catechol in the aniline ring (**26**, **29**–**32**) displayed moderate inhibitory activity (56%–65%). When the sulfonamide nitrogen was substituted by an aliphatic group, such as methyl, propyl, pentyl, or benzylic group (**29**–**32**), the inhibitory effect on PKL activity was conserved. Comparing **27** with **26**, we found that the presence of a hydroxy group in the *para* position is not required since the activity was preserved. However, the complete replacement of catechol or phenol by a simple aniline (**28**) resulted in a decreased inhibitory effect on the PKL activity (44%).

Furthermore, an inhibitory effect was found for **34** (41%), which contained a propyl substituent on the nitrogen, compared to **33** (29%), which included a methyl group. Similar results to those for compounds **26**–**34** were obtained for compounds **35**–**37**; however, with three catechol rings, compound **35** was the most potent inhibitor of this series

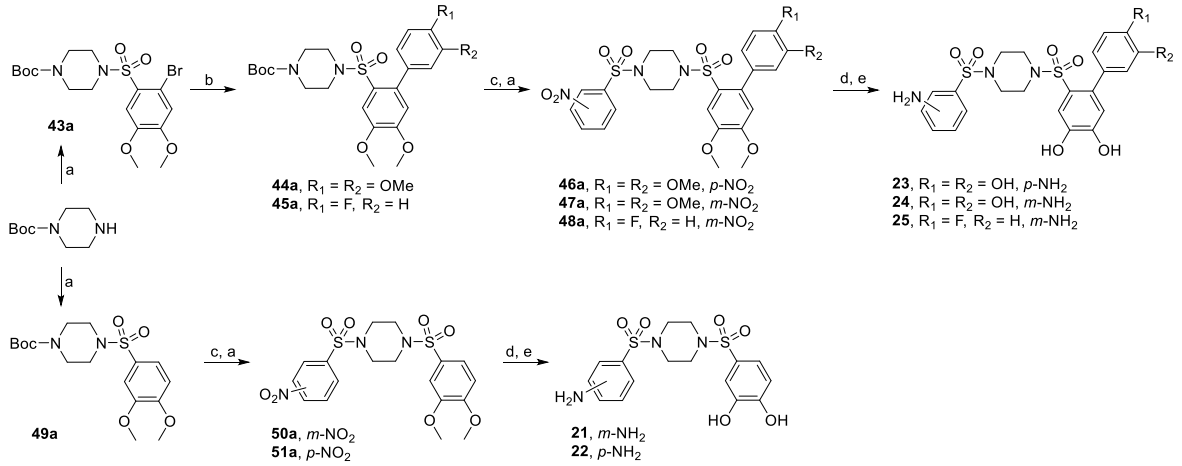

Scheme 2. Synthesis of DASA derivatives. *Reagents and conditions*. a) DIPEA, $ArSO_2Cl$, DCM, r.t, 1 h, 66–99%; b) $Pd(PPh_3)_4$, K_2CO_3, 120 °C, 1 h, tol:EtOH:H_2O, 83–95%; c) CF_3COOH, DCM, r.t, 30 min, 69–96%; d) Fe, NH_4Cl; EtOH:THF:H_2O, 60 °C, 8 h, 19–89%; e) BBr_3, DCM, 0 °C to r.t, 2 h, 11–49%; f) DIPEA, DCM, $BrCH_2Ar$, r.t, 16 h, 56-56-92%.

of compounds, with 81% inhibition of PKL. Similarly, **38**, a dimer of **35**, presented a more potent inhibitory effect (70%) than compounds with a ring that occupied only subpocket 1, such as **26**–**34**. The inhibitory capability of the most potent compound (**35**) was evaluated using purified PKL, resulting in IC_{50} of 120 nM (Fig. 4F). We next sought to understand the enzyme–inhibitor interactions that influence activity. Our attempts to crystallise this series of inhibitors resulted in poor diffracting crystals, suggesting that the compound induces a conformational change that is incompatible with our crystal form. We, therefore, undertook docking studies to establish the structure-activity relationships of these inhibitors by molecular docking in MOE using the crystal structure of PKL in a complex with **17** as our guide. The docked inhibitors were scored based on an *S*-score value, root mean square deviation (RMSD) between conformations, and similarity to the binding mode of **17** (Fig. 4E, F, G).

The docking simulation yielded relative binding free energies ranging from −6.92 to −11.33 kcal mol^{-1}, covering about 6 orders of predicted magnitude in binding affinity. Overall, the binding conformations were consistent, with RMSD values ranging from 1.15 to 2.54 Å (Table S1). The docked compounds generally maintained key interactions with Tyr402, Gln405, and other interactions, such as the π- π interaction between the two Phe38 side chains. Nevertheless, the docking studies revealed multiple positions where these derivatives could bind to PKL, contrasting with the first hybrid generation, which provided well-defined crystal structures with PKL. This suggests that compounds **26**–**38** might exhibit different binding modes within the allosteric site, potentially causing structural changes incompatible with the crystal form we used (Fig. 4E–G).

2.8. Removing the SO_2 group decreases the ability to activate PKL

Since the aromatic ring D in compounds **39**–**52** had such a significant effect on the activity of the ligands, we wanted to make further modifications to probe the importance of other chemical groups. Since the single-point concentration experiments indicated that the catechol moieties were essential for PKL modulation, these were retained in the new design. Visual analysis of the X-ray crystal structures of PKL in complex with **5** and **17** (Fig. 2E and F) suggested that the sulfone group of these ligands does not contribute to any significant hydrogen-bond interactions. By conjecture, the role of the sulfone group in binding could be to stabilise the position of the ligand between the aromatic rings of Phe38 by providing steric hindrance to “lock” the ligand in place. Following this reasoning, ligand efficacy would be expected to change drastically upon removing the sulfone bridge. To test this hypothesis, the sulfone group was replaced with a methylene bridge since molecular modelling suggests that this would allow the ligands to retain a similar conformation (Fig. 5A).

Additionally, to investigate the similarity of the SAR of the novel series to that of **39**–**52**, variants were synthesised both with and without the aromatic ring D, where the positions of the catechol groups were varied. Initially, **41** and **44** were made as close analogues of **5** and **17**, respectively. **42** and **45** were similarly analogous, with only the catechol of aromatic ring C removed. In compound **46**, the catechol on aromatic ring D was replaced by fluorine in the 4-position, while **47** included the same modification without the catechol on ring C. In addition to these compounds, several more diverse compounds with a more structural variation were synthesised, but without success in improving their effect on PKL (data not shown). The naphthalene derivative **43** was designed to increase lipophilicity, and **47** was methylated at the sulfonamide to evaluate the importance of the sulfonamide hydrogen.

The synthetic sequence started with the construction of the common nitrile intermediates **78a**–**79a** (Scheme 4A). The subsequent reactions proceeded with good-to-excellent yields for both precursors to generate the amine salts **80a** and **81a** as free-flowing solids. Amines **80a** and **81a** were then reacted with sulfonyl chlorides to incorporate ring C (Scheme 4B). Amide-containing compound **39** was obtained via hydrogenation of nitrated precursor **84a**. Compound **39** was then treated with refluxing HCl in 1,4-dioxane to generate the free amine **40**. Intermediates **85a**–**87a** were directly deprotected by treatment with BBr_3 to afford compounds **41**–**43**. The brominated intermediates **82a** and **83a** were reacted with aryl boronic acids under Suzuki-Miyaura reaction conditions to incorporate the final ring D (**88a**–**98a**). The final products **44**–**52** were obtained via methoxy deprotection using BBr_3.

2.9. Inhibitory effect on PKL activity by removing the SO_2 group

Interestingly, all the ligands in this series were moderate inhibitors (Fig. 5B), contrasting the activator-inhibitor duality of the parent compounds. This strongly suggests that sulfone provides some critical interaction with the protein; however, the nature of this still needs to be fully understood. Ligands **44**, **46**, **49**, and **51** inhibited PKL activity by 60%, 71%, 72%, and 68%, respectively, in cell lysate assays, suggesting that for this series of compounds, the substitution pattern of ring D does not remarkedly affect potency (Fig. 5B). A similar inhibitory effect on PKL activity in cell lysates was observed for compounds **41** and **44** (61% and 60%, respectively), indicating that the presence of ring D has a minor effect on the inhibition of this ligand series.

However, comparing linear ligands **41** with **5** shows that the

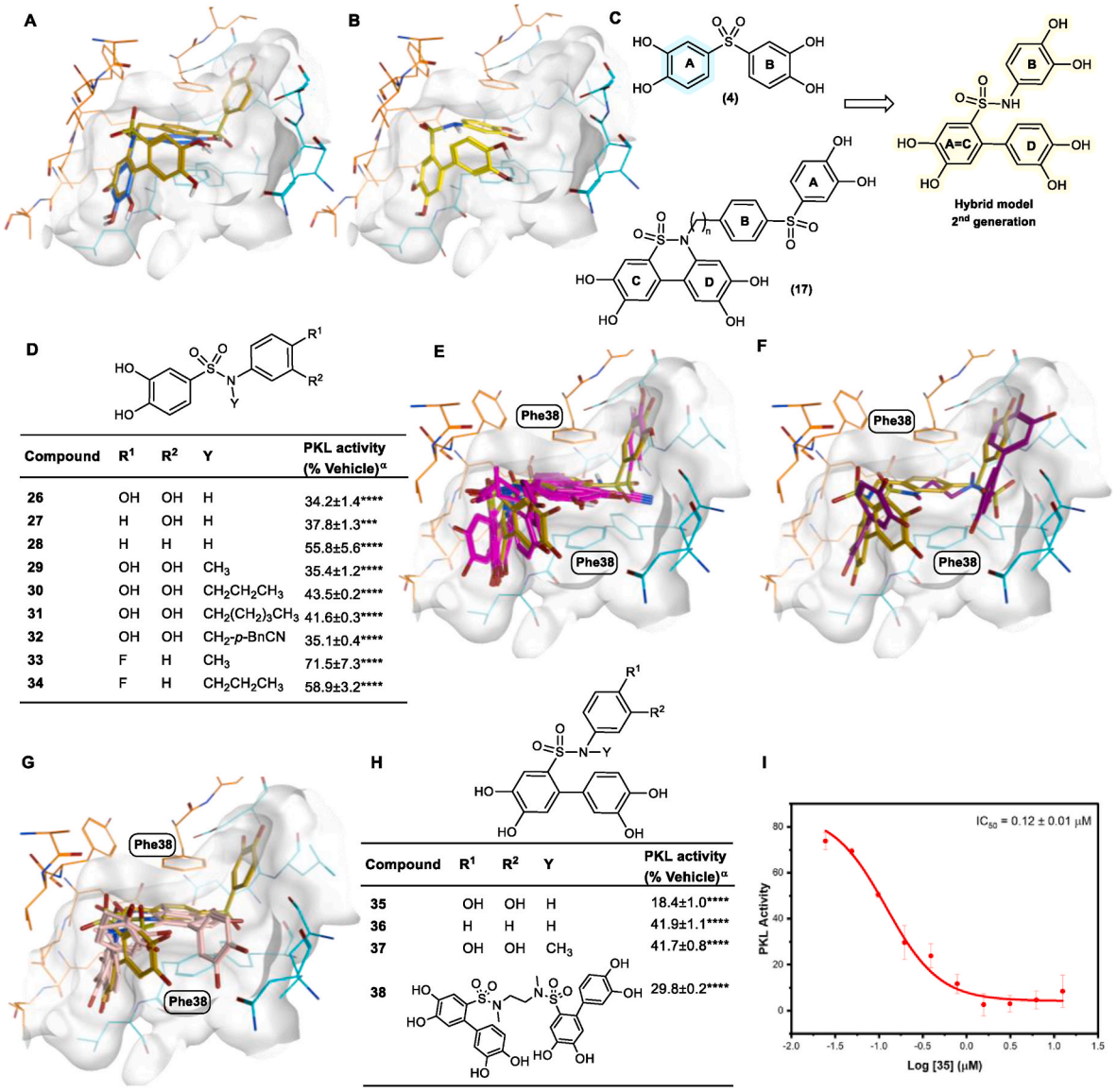

Compound	R^1	R^2	Y	PKL activity (% Vehicle)[α]
26	OH	OH	H	34.2±1.4****
27	H	OH	H	37.8±1.3***
28	H	H	H	55.8±5.6****
29	OH	OH	CH_3	35.4±1.2****
30	OH	OH	$CH_2CH_2CH_3$	43.5±0.2****
31	OH	OH	$CH_2(CH_2)_3CH_3$	41.6±0.3****
32	OH	OH	CH_2-*p*-BnCN	35.1±0.4****
33	F	H	CH_3	71.5±7.3****
34	F	H	$CH_2CH_2CH_3$	58.9±3.2****

Compound	R^1	R^2	Y	PKL activity (% Vehicle)[α]
35	OH	OH	H	18.4±1.0****
36	H	H	H	41.9±1.1****
37	OH	OH	CH_3	41.7±0.8****
38				29.8±0.2****

Fig. 4. Structural basis for the design of the second-generation hybrid model. **A**) Superposition of crystal structures of **17** (gold, PDB: 7FS5) and **4** (blue, PDB: 7FRV) in the cavity of the allosteric site. **B**) Model representation of the second-generation hybrid compound in the cavity of the allosteric site (in yellow). **C**) Proposed hybrid model in 2D – second generation based on **4** and **17**. **D, H**) Effect of compounds (**26**–**38**) on PKL activity in cell lysates, expressed as % of the PKL activity in the vehicle. Mean ± SD, n = 3, *p < 0.05, **p < 0.01, ***p < 0.001, ****p < 0.0001, One Way ANOVA followed by Dunnett's multiple comparison test. **E**) The docking positions of compounds **26**–**34** (fuchsia) overlaid with the complex crystal structure of **17** (gold) with PKL (PDB: 7FS5). **F**) same as (**E**) for compound **38** (purple). **G**) same as (**E**) for compounds **35**–**37** (pale pink). **I**) IC_{50} curve for compound **35**, mean ± SD, n = 3. [α]The compounds (10 μM) were incubated for 5 min at RT with cell lysates obtained from the HepG2 PKM2 KO liver cell line.

replacement of SO_2 with CH_2 increases the inhibitory effect. This suggests that the sulfone groups contribute primarily by providing steric hindrance rather than making hydrogen bonds. If any critical hydrogen bonds between the protein and the sulfone of **5** were present, the activity of **41** would be expected to decrease accordingly. The methoxy-bearing compounds (**85a**, **90a**, **92a**–**93a**, **95a**–**98a**) were utterly inert in the cell lysate assay. All the deprotected counterparts of these compounds were active in cell lysate assays, suggesting the importance of the catechol functional groups.

Similarly, the aniline analogues **39** and **40** were also inactive in cell lysate assays. These results indicate that the hydrogen-donating capability of the hydroxide groups is essential for ligand binding. Compounds **45** and **47** lacked the catechol group at ring C and consequently had lower activities than their analogues, **44** and **46**. This further proves that the catechol functionality of ring C is essential for ligand binding. Ligand **42** was slightly more active than its naphthalene analogue **43**.

In contrast to the remaining ligands, these contained a benzylic CH_2 group in place of the sulfonamide. The complete loss of activity strongly indicates that the sulfonamide group contributes an essential interaction with the protein, possibly by positioning the ligands between the two phenylalanines.

Three compounds analogous to **47** containing methoxy groups in rings A and C and halogen atoms at the *p*-position of ring D, namely F, Cl, and Br (**90a**–**92a**), showed moderate inhibitory effects on PKL activity after incubation with the liver cell line (between 12% and 35% inhibition). We observed higher levels of inhibition after longer incubation times and increased compound concentrations (Table S2). Compounds **42** and **44** were soaked with PKL, resulting in crystal structures of corresponding complexes (Fig. 5C and D). These structures show that lack of a sulfone group does not prevent binding of these molecules to the allosteric site, while not inducing allosteric effect on enzyme activity. The similarity between the binding poses of these ligands with their

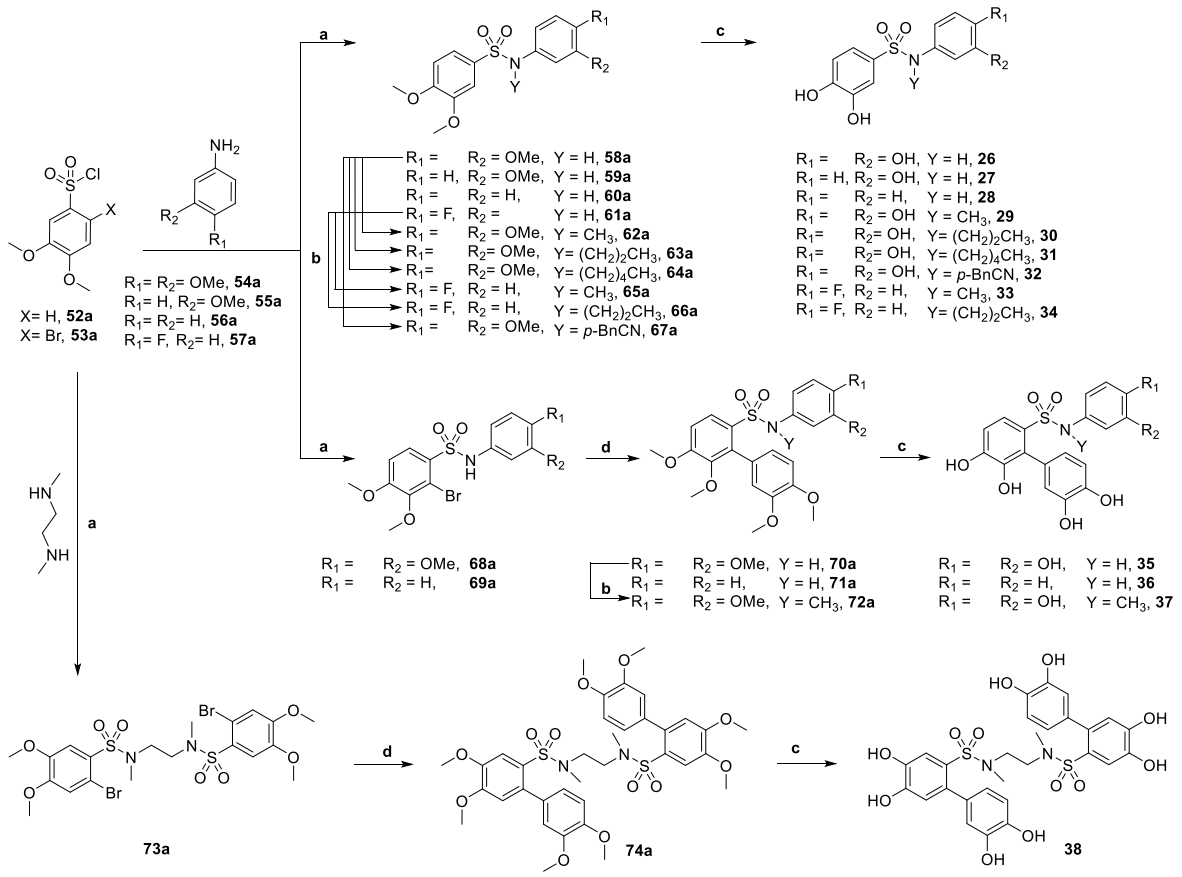

Scheme 3. Synthesis of second-generation hybrid compounds. *Reagents and conditions*. a) DIPEA, DCM, r.t, 1–24 h, 18–83%; b) MeCN, K_2CO_3, alkyl-halide, MW, 100 °C, 1 h, 29–98%; c) BBr_3, DCM, 1–5 h, 13–63%; d) $Pd(PPh_3)_4$, K_2CO_3, 3,4-dimethoxybenzeneboronioc acid, tol:EtOH:H_2O, 120 °C, MW, 1 h, 18–55%.

parent compounds, **5** and **11**, respectively, is further proof of the steric role of the sulfone groups.

3. Conclusion

We have developed a series of pyruvate kinase modulators that inhibit or activate the enzyme. We describe the design and synthesis of 42 first-in-class compounds, and we have assessed the effects of 48 compounds on PKL activity through *in vitro* assays using cell lysates obtained from a liver cell line. We discovered that the structure of small molecules affects their ability to activate or inhibit PKL activity via the same allosteric site. These preliminary results pave the way for new studies to understand how an allosteric binding site can enable both positive and negative regulation of enzyme activity. Among the series of compounds presented here, 17 were confirmed to bind in the allosteric site of PKL through X-ray crystallography. Combining the cell lysate effects on PKL activity by the designed compounds and the X-ray structures of them bound to PKL generated a structure–activity-relationship (Fig. 6).

The symmetry in the allosteric site of PKL allowed the pocket to be filled with compounds containing arylsulfonamides or arylsulfones, which generate the activation of PKL (**5**–**8**; **10**; **21**, **22**). To generate an inhibitory effect on the PKL activity, two main structural characteristics were observed: first, the introduction of substituents on the sulfonamide group to fill subpocket 2, thus breaking the symmetry in subpocket 1 (**11, 12; 15, 16; 17; 19; 20; 23**–**25; 26**–**38**); and second, replacing the sulfone group by a methylene group, thereby decreasing the lipophilic interaction with Tyr402 (**44**–**52**). Interaction with Asp366 appears necessary for inhibition since compounds **13**, **14** and **18** lack hydroxyl in position R1, which makes water-mediated interaction with Asp366 (Figs. S1–S2 for **13** and **18**). The crystal structure of **20** (Scheme 1D) shows the occupancy of subpocket 2 by an aryl group connected to the tertiary amine. These results suggest that small substituents, such as the acetyl group in **19** or the introduction of ring D (**11**, **12**, **15**, **16**, **17**), are sufficient to occupy subpocket 2 and cause an inhibitory effect.

The M2 and R isoforms of pyruvate kinase are well known to present compounds that activate the PK activity, but no reports are found for PKL. Our assumptions about the allosteric regulation of PKL resulted in the fantastic effect of this class of hybrid compounds in the activity of the enzyme. The results presented in this work are the beginning of exploring this class of modulators to understand the biological implications that this allosteric site is made for and, so far, is unexplored.

4. Experimental section

4.1. Chemical synthesis and characterisation

4.1.1. General information

Unless otherwise specified, all reagents were obtained from commercial supplier Sigma-Aldrich and used without further purification. Solvents were dried on a solvent purification system (PS-MD-5/7 Inert technology). Those reactions that employed microwave irradiation were performed in capped vials using a Biotage Initiator + system. Reactions were monitored by LC-MS (PerkinElmer Series 200; Waters Symmetry C8 column 3.5 μm, 4.6 × 50 mm; water:CH_3CN (0.1% formic acid)) or by thin-layer chromatography (TLC) on silica-gel-coated aluminium foils (silica gel 60 F254, Merck). The TLC plates were visualized by UV light (λ = 254 nm). Flash-column chromatography was performed on an Isolera One or Selekt flash chromatography systems (Biotage), using silica gel SNAP KP-Sil, Sfär cartridges or reversed phase Sfär C18

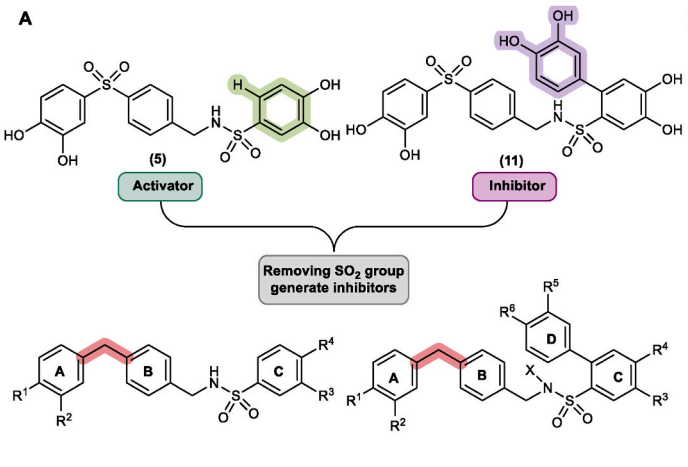

B

Compound	R^1	R^2	R^3	R^4	R^5	R^6	Y	PKL activity (% Vehicle)[α]
39	NHAc	H	NH_2	H	-	-	-	no effect
40	NH_2	H	NH_2	H	-	-	-	no effect
41	OH	OH	OH	OH	-	-	-	39.2±0.9****
42	OH	OH	H	H	-	-	-	40.9±1.2***
43	OH	OH	*	*	-	-	-	45.4±1.9****
44	OH	OH	OH	OH	OH	OH	H	39.7±0.9***
45	OH	OH	OH	H	OH	OH	H	50.8±0.4****
46	OH	OH	OH	OH	H	F	H	29.3±1.2****
47	OH	OH	H	H	H	F	H	43.7±1.6****
48	OH	OH	H	H	H	F	CH_3	40.3±0.8****
49	OH	OH	OH	OH	H	$CONH_2$	H	28.5±1.0****
50	OH	OH	OH	OH	H	H	H	50.0±2.7****
51	OH	OH	OH	OH	H	CO_2Me	H	31.7±0.4****
52	OH	OH	H	H	H	$CONH_2$	H	58.5±2.4****

* ring-C= 2-naphtyl

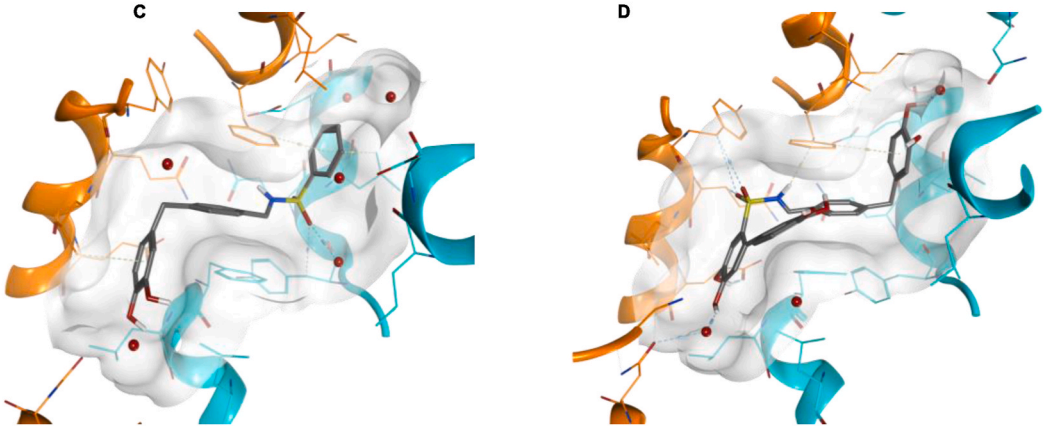

Fig. 5. Design of third-generation model. **A**) New model based on activator **5** and inhibitor **11** by replacement of the SO_2 group with a CH_2 chain. **B**) Effect of compounds **39**–**52** on PKL activity in cell lysates expressed as % of the PKL activity in the vehicle. Mean ± SD, n = 3, *p < 0.05, **p < 0.01, ***p < 0.001, ****p < 0.0001, One Way ANOVA followed by Dunnett's multiple comparison test. **C, D**) Inhibitors bound to PKL in the allosteric site of the A–A interface; binding site of compound **42** (PDB: 7FSC) and compound **44** (PDB: 7FSD). [α]The compounds (10 μM) were incubated for 5 min at RT with cell lysates obtained from the HepG2 PKM2 KO liver cell line.

columns. Melting points were determined with a Büchi B-545 apparatus. NMR spectra were recorded on a Varian NMR 400 spectrometer at 25 °C. All chemical shifts are reported in parts per million (δ) relative to the residual solvent peak. The following abbreviations are used to denote signal patterns: (s) singlet, (d) doublet, (t) triplet, (q) quartet, (m) multiplet, and (br) broad, unless otherwise noted. Coupling constants (*J*) are reported in Hertz (Hz). High resolution mass spectra (HRMS) were recorded on an Agilent 1290 infinity LC system tandem to an Agilent 6520 Accurate Mass Q-TOF spectrometer.

Intermediate compounds. Detailed synthesis procedures of intermediates are described in the Supplementary Information.

4.2. General procedure A – demethylation by boron tribromide

To a stirred solution of the selected methoxy protected sulfonamide in DCM (5 mL) at 0 °C boron tribromide (1.5–2.0 equiv. per OMe group) was added dropwise and the solution was gradually allowed to heat back to 19 °C and monitored until complete deprotection by LCMS or TLC. The reaction was quenched by adding H_2O dropwise with the reaction vessel at 0 °C, until fuming stopped and then an excess was added (10 mL). The organic layer was separated, concentrated, diluted with EtOAc (10 mL), and washed with H_2O (2 × 10 mL). The combined aqueous phase was extracted with EtOAc (10 mL), and the combined organic phase was washed with brine (10 mL), dried over Na_2SO_4, gravity filtered, concentrated, mounted on silica and purified by flash chromatography to afford the desired hydroxyl product.

4.3. General procedure B – N-Boc deprotection

To a solution of the selected sulfonamide in DCM (5 mL) trifluoroacetic acid (200 equiv.) was added, and the reaction mixture was left to stirred for 2 h at room temperature. The solvent is evaporated to dryness and the residue is diluted with EtOAc (10 mL), washed three times with H_2O (3 × 10 mL), the combined organic phase was washed with brine (10 mL), dried over Na_2SO_4, filtered, concentrated, mounted on silica and purified by flash chromatography to afford the desired compound.

4.4. General procedure C – nitro reduction with iron

To a solution of nitro compound in THF (3 mL) and EtOH (3 mL) was added ammonium chloride (1.5 equiv.) in water (3 mL) and Iron (3.0 equiv.). The reaction mixture was stirred at 60 °C and monitored by TLC until complete reduction. The reaction was allowed to cool to room temperature and the heterogeneous mixture was filtered through a bed of Celite, the cake was washed with EtOAc. The solution was concentrated to half-volume, then diluted with EtOAc (25 mL) and 1 N NaOH (50 mL). The organic layer was separated. Aqueous phase was extracted with EtOAc (2 × 20 mL). The organic phase was combined, dried over Na_2SO_4, filtered, and concentrated, mounted on silica and purified by flash chromatography to afford the desired compound.

4.4.1. N-(4-((3,4-Dihydroxyphenyl)sulfonyl)benzyl)-3,4-dihydroxybenzenesulfonamide (5)

Following general procedure A, **34a** (190 mg, 0.37 mmol) was

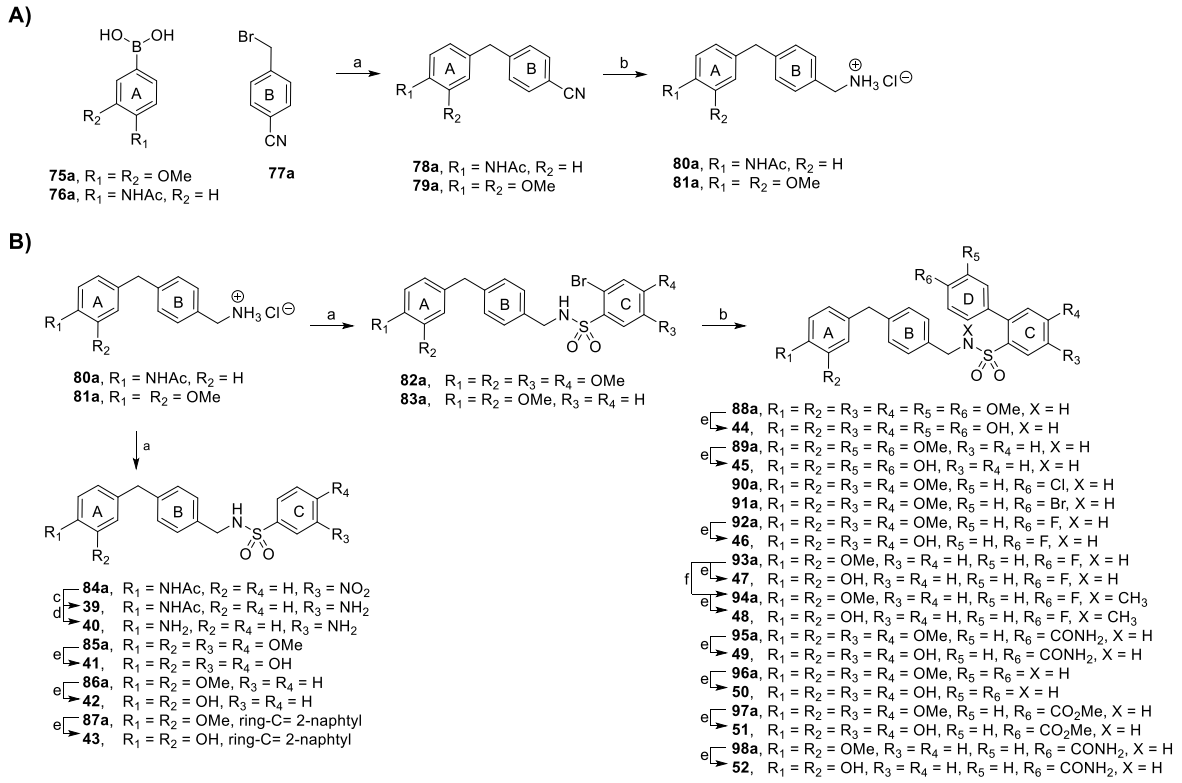

Scheme 4. Synthesis of hybrid inhibitors. *Reagents and conditions*. **A**) a) $Pd(PPh_3)_4$, K_2CO_3, tol:EtOH:H_2O (5:2:1), 80 °C, 2 h, 92–94%; b) H_2, Pd, HCl, MeOH:DCM, r.t, 3–24 h, 68–99%; **B**) a) $ArSO_2Cl$, DMF, 1 h, 49–87%; b) $Pd(PPh_3)_4$, K_2CO_3, tol:EtOH:H_2O (5:2:1), 80 °C, 2 h, 92–94%; c) Pd/C, MeOH, H_2, r.t, 2 h min, 87%; d) HCl (4 M), 1,4-dioxane, reflux, 2 h, 21–87%; e) BBr_3, DCM, 0 °C to r.t, 2 h, 9–91%; f) MeI, Na_2CO_3, MeCN, 100 °C, 2 h.

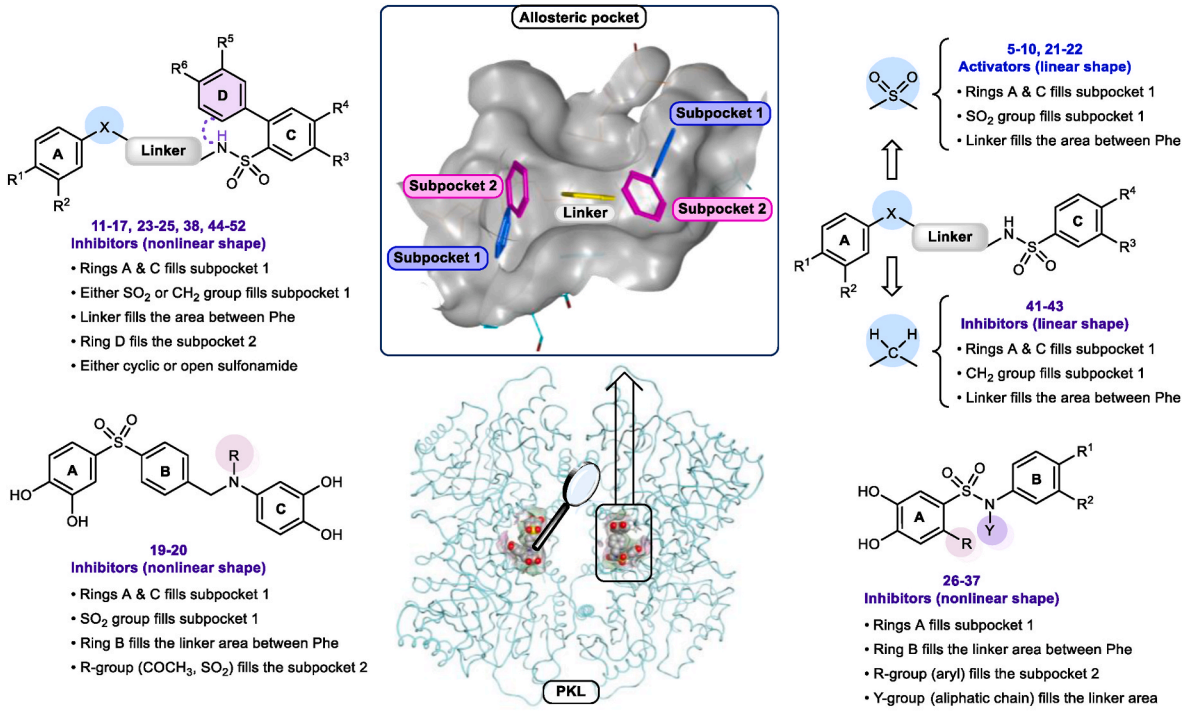

Fig. 6. Structure-activity relationship. Key structural features of each different series of designed compounds and presented in this work for the modulation of the PKL activity by the allosteric site.

reacted to afford 100 mg (59%) of the title compound as a white solid after column chromatography (DCM/MeOH 10%). mp: 80–81 °C. ^{1}H NMR (400 MHz, CD_3OD) δ 7.77 (d, J = 8.4 Hz, 2H), 7.41 (d, J = 8.2 Hz, 2H), 7.30–7.25 (m, 2H), 7.23 (d, J = 2.2 Hz, 1H), 7.18 (dd, J = 8.3, 2.1 Hz, 1H), 6.86 (dd, J = 13.2, 8.3 Hz, 2H), 4.06 (s, 2H). ^{13}C NMR (101 MHz, CD_3OD) δ 151.92, 151.00, 147.07, 146.77, 144.84, 142.81,

132.73, 131.83, 129.77, 129.40, 128.44, 128.08, 121.75, 120.88, 116.50, 116.43, 116.02, 115.12, 68.85.

4.4.2. N-(4-((3,4-Dihydroxyphenyl)sulfonyl)phenethyl)-3,4-dihydroxybenzenesulfonamide (6)

Following general procedure A, **35a** (125 mg, 0.24 mmol) was reacted to afford 54 mg (48%) of the title compound as a white-off solid after column chromatography (DCM/MeOH 10%). mp: 79–81 °C. ^{1}H NMR (400 MHz, CD_3OD) δ 7.77 (d, J = 8.3 Hz, 2H), 7.33 (d, J = 8.3 Hz, 2H), 7.29 (dd, J = 8.3, 2.3 Hz, 1H), 7.26 (d, J = 2.3 Hz, 1H), 7.20 (d, J = 2.2 Hz, 1H), 7.15 (dd, J = 8.3, 2.2 Hz, 1H), 6.91–6.82 (m, 2H), 3.07 (t, J = 7.1 Hz, 2H), 2.79 (t, J = 7.1 Hz, 2H). ^{13}C NMR (101 MHz, CD_3OD) δ 151.81, 150.87, 147.00, 146.68, 146.06, 141.80, 132.85, 131.82, 130.84, 128.27, 121.55, 120.70, 116.44, 116.08, 115.24, 114.96, 44.80, 36.67. HRMS (*m/z*): [M]+ calcd. for $C_{20}H_{19}NO_8S_2$, 466.063; found, 466.0622.

4.4.3. 3,4-Dihydroxy-N-(4-((3-hydroxyphenyl)sulfonyl)benzyl)benzenesulfonamide (7)

Following general procedure A, **36a** (226 mg, 0.47 mmol) was reacted to afford 155 mg (75%) of the title compound as a beige solid after column chromatography (DCM/MeOH 10%). mp: 64–65 °C. ^{1}H NMR (400 MHz, CD_3OD) δ 7.82 (d, J = 8.4 Hz, 2H), 7.44 (d, J = 8.2 Hz, 2H), 7.39–7.31 (m, 2H), 7.28 (q, J = 1.5 Hz, 1H), 7.23 (d, J = 2.2 Hz, 1H), 7.18 (dd, J = 8.3, 2.3 Hz, 1H), 7.00 (dt, J = 6.0, 2.7 Hz, 1H), 6.84 (d, J = 8.3 Hz, 1H), 4.07 (s, 2H). ^{13}C NMR (101 MHz, CD_3OD) δ 159.54, 150.99, 146.75, 145.39, 143.82, 141.77, 131.81, 131.70, 129.68, 128.67, 121.55, 120.77, 119.32, 116.07, 114.97, 114.85, 47.17.

4.4.4. 3,4-Dihydroxy-N-(4-((3-hydroxyphenyl)sulfonyl)phenethyl)benzenesulfonamide (8)

Following general procedure A, **37a** (260 mg, 0.53 mmol) was reacted to afford 170 mg (72%) of the title compound as a white-off solid after column chromatography (DCM/MeOH 10%). mp: 82–84 °C. ^{1}H NMR (400 MHz, CD_3OD) δ 7.79 (d, J = 8.1 Hz, 2H), 7.38–7.27 (m, 5H), 7.22 (d, J = 2.2 Hz, 1H), 7.17 (dd, J = 8.3, 2.2 Hz, 1H), 7.00 (dt, J = 6.4, 2.5 Hz, 1H), 6.86 (d, J = 8.3 Hz, 1H), 3.05 (t, J = 7.1 Hz, 2H), 2.76 (t, J = 7.1 Hz, 2H). ^{13}C NMR (101 MHz, CD_3OD) δ 159.56, 150.92, 146.74, 146.69, 144.00, 140.92, 131.87, 131.67, 131.02, 128.74, 121.49, 120.69, 119.29, 116.08, 114.99, 114.85, 44.79, 36.74. HRMS (*m/z*): [M]+ calcd. for $C_{20}H_{19}NO_7S_2$, 450.0681; found, 450.0678.

4.4.5. N-(4-((4-Aminophenyl)sulfonyl)benzyl)-4-nitrobenzenesulfonamide (9)

Following general procedure B, **38a** (100 mg, 0.18 mmol) was reacted to afford 50 mg (61%) of the title compound as a white-off solid without further purification. mp: 204–206 °C. ^{1}H NMR (400 MHz, DMSO-d_6) δ 8.41–8.32 (m, 2H), 8.03–7.98 (m, 2H), 7.75–7.69 (m, 2H), 7.52–7.47 (m, 2H), 7.41–7.37 (m, 2H), 6.62–6.57 (m, 2H), 6.16 (s, 1H), 4.11 (s, 2H). ^{13}C NMR (101 MHz, DMSO-d_6) δ 153.56, 149.51, 146.06, 142.19, 129.37, 128.42, 128.08, 126.52, 125.19, 124.53, 112.95, 112.90, 45.47. HRMS (*m/z*): [M]+ calcd. for $C_{19}H_{17}N_3O_6S_2$, 448.0637; found, 448.0632.

4.4.6. 4-Amino-N-(4-((4-aminophenyl)sulfonyl)benzyl)benzenesulfonamide (10)

Following general procedure C, **38a** (290 mg, 0.53 mmol) was reacted to afford *tert*-butyl (4-((4-(((4-aminophenyl)sulfonamido)methyl)phenyl)sulfonyl)phenyl)carbamate, which was treated following general procedure E, this afford 80 mg (36%) of the title compound as a beige solid after column chromatography (pentane/EtOAc 50–100%). mp: 208–210 °C. ^{1}H NMR (400 MHz, DMSO-d_6) δ 7.75 (d, J = 8.4 Hz, 2H), 7.71 (t, J = 6.4 Hz, 1H), 7.51 (d, J = 8.8 Hz, 2H), 7.48–7.34 (m, 4H), 6.67–6.55 (m, 4H), 6.15 (s, 2H), 5.94 (s, 2H), 3.91 (d, J = 6.3 Hz, 2H). ^{13}C NMR (101 MHz, DMSO-d_6) δ 153.57, 152.57, 143.29, 141.91, 129.36, 128.47, 128.30, 126.45, 125.42, 125.21, 112.96, 112.67, 45.49. HRMS (*m/z*): [M]+ calcd. for $C_{19}H_{19}N_3O_4S_2$, 418.0895; found, 418.0892.

4.4.7. N-(3,4-Dihydroxyphenyl)-N-(4-((3,4-dihydroxyphenyl)sulfonyl)benzyl)-3,4-dihydroxybenzenesulfonamide (11)

Following general procedure A, **26a** (260 mg, 0.40 mmol) was reacted to afford 190 mg (84%) of the title compound as a white solid after column chromatography (DCM/MeOH 10%). ^{1}H NMR (400 MHz, CD_3OD) δ 7.77–7.73 (m, 2H), 7.46 (s, 1H), 6.87 (d, J = 8.3 Hz, 1H), 6.84 (d, J = 2.1 Hz, 1H), 6.72 (d, J = 8.1 Hz, 1H), 6.67 (s, 1H), 6.62 (dd, J = 8.1, 2.1 Hz, 1H), 3.81 (s, 2H). ^{13}C NMR (101 MHz, CD_3OD) δ 151.94, 150.07, 147.08, 146.30, 145.63, 145.20, 144.62, 142.82, 135.11, 132.74, 132.17, 129.75, 129.65, 128.24, 122.31, 121.61, 120.34, 118.20, 117.41, 116.48, 115.78, 115.29, 47.07. Data matches according with previous report [26].

4.4.8. N-(4-((3,4-Dihydroxyphenyl)sulfonyl)phenethyl)-3′,4,4′,5-tetrahydroxy-[1,1′-biphenyl]-2-sulfonamide (12)

Following general procedure A, **27a** (12 mg, 0.18 mmol) was reacted to afford 60 mg (57%) of the title compound as a white solid after column chromatography (DCM/MeOH 10%). ^{1}H NMR (400 MHz, CD_3OD) δ 7.76 (d, J = 8.5 Hz, 2H), 7.42 (s, 1H), 7.28 (dd, J = 8.3, 2.3 Hz, 1H), 7.25 (dd, J = 5.4, 3.2 Hz, 3H), 6.86 (d, J = 8.3 Hz, 1H), 6.81 (d, J = 2.1 Hz, 1H), 6.73 (d, J = 8.1 Hz, 1H), 6.66 (s, 1H), 6.63 (dd, J = 8.1, 2.1 Hz, 1H), 2.83 (t, J = 7.2 Hz, 2H), 2.64 (t, J = 7.2 Hz, 2H). ^{13}C NMR (101 MHz, CD_3OD) δ 151.81, 149.93, 146.97, 146.25, 145.69, 145.60, 145.16, 141.80, 134.84, 132.76, 132.08, 130.68, 129.45, 128.31, 122.10, 121.58, 120.19, 117.98, 117.25, 116.45, 115.78, 115.25, 44.55, 36.54. Data matches according with previous report [26].

4.4.9. 3′,4,4′,5-Tetrahydroxy-N-(4-((3-hydroxyphenyl)sulfonyl)benzyl)-[1,1′-biphenyl]-2-sulfonamide (13)

Following general procedure A, **28a** (150 mg, 0.24 mmol) was reacted to afford 29 mg (22%) of the title compound as a beige solid after column chromatography (DCM/MeOH 10%). mp: 110–111 °C. ^{1}H NMR (400 MHz, CD_3OD) δ 7.79 (d, J = 8.4 Hz, 2H), 7.46 (s, 1H), 7.36–7.34 (m, 2H), 7.33–7.30 (m, 2H), 7.28 (dt, J = 2.3, 0.8 Hz, 1H), 7.01–6.98 (m, 1H), 6.84 (d, J = 2.1 Hz, 1H), 6.72 (d, J = 8.1 Hz, 1H), 6.67 (s, 1H), 6.63–6.61 (m, 1H), 3.82 (s, 2H). ^{13}C NMR (101 MHz, CD_3OD) δ 159.54, 150.05, 146.26, 145.60, 145.17, 143.83, 141.77, 135.09, 132.15, 131.70, 129.74, 129.72, 128.64, 122.31, 121.55, 120.34, 119.32, 118.18, 117.40, 115.77, 114.85, 47.03.

4.4.10. 3′,4,4′,5-tetrahydroxy-N-(4-((3-hydroxyphenyl)sulfonyl)phenethyl)-[1,1′-biphenyl]-2-sulfonamide (14)

Following general procedure A, **29a** (120 mg, 0.19 mmol) was reacted to afford 23 mg (22%) of the title compound as a beige solid after column chromatography (DCM/MeOH 10%). mp: 88–90 °C. ^{1}H NMR (400 MHz, CD_3OD) δ 7.79 (d, J = 8.4 Hz, 2H), 7.43 (s, 1H), 7.35 (d, J = 5.4 Hz, 2H), 7.30–7.23 (m, 3H), 7.02–6.97 (m, 1H), 6.81 (d, J = 2.1 Hz, 1H), 6.73 (d, J = 8.1 Hz, 1H), 6.67 (s, 1H), 6.63 (dd, J = 8.1, 2.1 Hz, 1H), 2.83 (t, J = 7.2 Hz, 2H), 2.64 (t, J = 7.2 Hz, 2H). ^{13}C NMR (101 MHz, CD_3OD) δ 159.53, 149.98, 146.31, 145.66, 145.21, 143.92, 140.91, 134.87, 132.13, 131.67, 130.85, 129.52, 128.79, 122.14, 121.51, 120.21, 119.32, 118.01, 117.28, 115.78, 114.85, 44.53, 36.61. HRMS (*m/z*): [M]+ calcd. for $C_{26}H_{23}NO_9S_2$, 558.0892; found, 558.0889.

4.4.11. N-(4-((3,4-Dihydroxyphenyl)sulfonyl)benzyl)-4,4′,5-trihydroxy-[1,1′-biphenyl]-2-sulfonamide (15)

Following general procedure A, **30a** (160 mg, 0.26 mmol) was reacted to afford 28 mg (28%) of the title compound as a beige solid after column chromatography (DCM/MeOH 10%). mp: 144–146 °C. ^{1}H NMR (400 MHz, CD_3OD) δ 7.74 (d, J = 8.1 Hz, 2H), 7.48 (s, 1H), 7.27 (td, J = 7.2, 6.1, 2.3 Hz, 4H), 7.13–7.03 (m, 2H), 6.87 (d, J = 8.2 Hz, 1H), 6.78–6.68 (m, 2H), 6.63 (s, 1H), 3.82 (s, 2H). ^{13}C NMR (101 MHz, CD_3OD) δ 158.19, 151.95, 150.10, 147.09, 145.17, 144.66, 142.80,

135.18, 132.72, 131.96, 131.64, 129.99, 129.65, 128.18, 121.60, 120.52, 117.50, 116.49, 115.55, 115.26, 46.92. HRMS (*m/z*): [M]+ calcd. for $C_{25}H_{21}NO_9S_2$, 544.0736; found, 544.0736.

4.4.12. 4,4′,5-Trihydroxy-N-(4-((3-hydroxyphenyl)sulfonyl)benzyl)-[1,1′-biphenyl]-2-sulfonamide (16)

Following general procedure A, **31a** (140 mg, 0.24 mmol) was reacted to afford 39 mg (31%) of the title compound as a beige-brownish solid after column chromatography (DCM/MeOH 10%). mp: 78–80 °C. ^{1}H NMR (400 MHz, CD_3OD) δ 7.78 (d, *J* = 8.0 Hz, 2H), 7.48 (s, 1H), 7.40–7.21 (m, 5H), 7.09 (d, *J* = 8.2 Hz, 2H), 7.00 (dd, *J* = 6.0, 3.0 Hz, 1H), 6.73 (d, *J* = 8.0 Hz, 2H), 6.63 (s, 1H), 3.83 (s, 2H). ^{13}C NMR (101 MHz, CD_3OD) δ 159.55, 158.16, 150.11, 145.22, 145.16, 143.81, 141.75, 135.17, 131.95, 131.72, 131.63, 129.95, 129.75, 128.59, 121.58, 120.52, 119.31, 117.49, 115.55, 114.85, 46.88. HRMS (*m/z*): [M]+ calcd. for C25H21NO8S2, 528.0787; found, 528.0786.

4.4.13. 6-(4-((3,4-Dihydroxyphenyl)sulfonyl)benzyl)-2,3,8,9-tetrahydroxy-6H-dibenzo [c,e] [1,2]thiazine 5,5-dioxide (17)

Following general procedure A, **32a** (170 mg, 0.26 mmol) was reacted to afford 81 mg (55%) of the title compound as a beige solid after column chromatography (DCM/MeOH 10%). ^{1}H NMR (400 MHz, CD_3OD) δ 7.71–7.65 (m, 2H), 7.30 (d, *J* = 8.1 Hz, 2H), 7.25 (dq, *J* = 4.3, 2.3 Hz, 2H), 7.18 (d, *J* = 15.1 Hz, 2H), 7.06 (s, 1H), 6.88 (d, *J* = 8.9 Hz, 1H), 6.59 (s, 1H), 4.83 (s, 2H). ^{13}C NMR (101 MHz, CD_3OD) δ 151.92, 151.10, 147.69, 146.98, 146.34, 145.32, 143.07, 142.97, 132.47, 132.02, 129.93, 129.62, 128.23, 127.85, 127.15, 126.58, 121.82, 119.72, 116.52, 115.40, 112.11, 111.99, 110.84, 109.84, 54.58. Data matches according with previous report [26].

4.4.14. 6-(4-((3,4-Dihydroxyphenyl)sulfonyl)phenethyl)-2,3,8,9-tetrahydroxy-6H-dibenzo [c,e] [1,2]thiazine 5,5-dioxide (18)

Following general procedure A, **33a** (100 mg, 0.15 mmol) was reacted to afford 42 mg (48%) of the title compound as a dark beige solid after column chromatography (DCM/MeOH 10%). ^{1}H NMR (400 MHz, CD_3OD) δ 7.62 (d, *J* = 8.5 Hz, 2H), 7.27–7.22 (m, 2H), 7.18 (s, 1H), 7.15–7.09 (m, 4H), 6.87 (d, *J* = 8.4 Hz, 1H), 6.75 (s, 1H), 3.93 (t, *J* = 7.3 Hz, 2H), 2.74 (t, *J* = 7.3 Hz, 2H). ^{13}C NMR (101 MHz, CD_3OD) δ 151.82, 151.09, 147.87, 146.96, 146.39, 145.25, 145.24, 141.72, 132.77, 131.75, 130.71, 128.06, 127.14, 126.98, 121.61, 119.99, 116.49, 115.26, 112.18, 111.81, 111.37, 111.14, 109.50, 52.04, 34.87. Data matches according with previous report [26].

4.4.15. N-(3,4-Dihydroxyphenyl)-N-(4-((3,4-dihydroxyphenyl)sulfonyl)benzyl)acetamide (19)

Following general procedure A, **41a** (310 mg, 0.64 mmol) was reacted to afford 200 mg (73%) of the title compound as a beige solid after column chromatography (DCM/MeOH 10%). mp: 112–114 °C. ^{1}H NMR (400 MHz, CD_3OD) δ 7.79 (d, *J* = 8.5 Hz, 2H), 7.38 (d, *J* = 7.8 Hz, 2H), 7.30–7.25 (m, 2H), 6.87 (d, *J* = 8.3 Hz, 1H), 6.70 (d, *J* = 8.3 Hz, 1H), 6.47 (d, *J* = 2.5 Hz, 1H), 6.40 (dd, *J* = 8.3, 2.5 Hz, 1H), 4.84 (s, 2H), 1.88 (s, 3H). ^{13}C NMR (101 MHz, CD_3OD) δ 173.63, 151.95, 147.13, 147.09, 146.72, 144.48, 142.87, 135.43, 132.71, 130.40, 128.32, 121.63, 120.20, 116.63, 116.48, 115.77, 115.30, 53.64, 22.31.

4.4.16. N-(3,4-Dihydroxyphenyl)-N-(4-((3,4-dihydroxyphenyl)sulfonyl)benzyl)-3,4-dihydroxybenzenesulfonamide (20)

Following general procedure A, **40a** (390 mg, 0.61 mmol) was reacted to afford 200 mg (59%) of the title compound as a pale-purple solid after column chromatography (DCM/MeOH 10%). mp: 90–92 °C. ^{1}H NMR (400 MHz, CD_3OD) δ 7.78–7.72 (m, 2H), 7.45–7.40 (m, 2H), 7.29–7.22 (m, 2H), 7.08–7.02 (m, 2H), 6.87 (dd, *J* = 8.3, 4.0 Hz, 2H), 6.56 (d, *J* = 8.5 Hz, 1H), 6.42 (d, *J* = 2.5 Hz, 1H), 6.28 (dd, *J* = 8.5, 2.5 Hz, 1H), 4.68 (s, 2H). ^{13}C NMR (101 MHz, CD_3OD) δ 151.95, 151.43, 147.06, 146.61, 146.44, 146.24, 144.04, 142.89, 132.59, 131.95, 130.38, 129.57, 128.15, 121.71, 121.63, 121.48, 117.42, 116.46, 116.04, 115.85, 115.76, 115.28, 55.48. HRMS (*m/z*): [M]+ calcd. for $C_{25}H_{21}NO_{10}S_2$, 560.0685; found, 560.0697.

4.4.17. 4-((4-((3-Aminophenyl)sulfonyl)piperazin-1-yl)sulfonyl)benzene-1,2-diol (21)

Following general procedure C, **50a** (300 mg, 0.64 mmol) was reacted to afford 58 mg (21%) of 3-((4-((3,4-dimethoxyphenyl)sulfonyl)piperazin-1-yl)sulfonyl)aniline as a white solid after column chromatography (pentane/EtOAc 50–100%). ^{1}H NMR (400 MHz, DMSO-d_6) δ 7.27 (dd, *J* = 8.4, 2.2 Hz, 1H), 7.20 (d, *J* = 7.8 Hz, 1H), 7.15 (d, *J* = 8.6 Hz, 1H), 7.07 (d, *J* = 2.1 Hz, 1H), 6.85 (t, *J* = 2.0 Hz, 1H), 6.80 (dd, *J* = 8.1, 2.0 Hz, 1H), 6.73 (dd, *J* = 7.6, 1.6 Hz, 1H), 3.86 (s, 3H), 3.82 (s, 3H), 2.96 (p, *J* = 4.8 Hz, 8H). ^{13}C NMR (101 MHz, DMSO-d_6) δ 152.73, 149.58, 148.82, 135.38, 129.75, 126.31, 121.38, 118.13, 113.85, 111.51, 111.39, 109.82, 55.94, 55.87, 45.11. Following general procedure A, 3-((4-((3,4-dimethoxyphenyl)sulfonyl)piperazin-1-yl)sulfonyl)aniline (50 mg, 0.11 mmol) was reacted to afford 23 mg (49%) of title compound as pale pink solid after reverse phase column chromatography (H_2O/MeCN 20–50%). mp: 204–206 °C. ^{1}H NMR (400 MHz, DMSO-d_6) δ 7.22 (t, *J* = 7.9 Hz, 1H), 7.06–6.95 (m, 2H), 6.90 (d, *J* = 8.3 Hz, 1H), 6.86 (d, *J* = 2.0 Hz, 1H), 6.82 (dd, *J* = 8.0, 2.3 Hz, 1H), 6.74 (dd, *J* = 8.0, 1.7 Hz, 1H), 5.64 (s, 2H), 2.92 (dd, *J* = 20.2, 5.1 Hz, 8H). ^{13}C NMR (101 MHz, DMSO-d_6) δ 150.44, 149.62, 145.60, 135.30, 129.75, 124.23, 119.94, 118.12, 115.56, 114.40, 113.84, 111.49, 45.23, 45.18. HRMS (*m/z*): [M]+ calcd. for $C_{16}H_{19}N_3O_6S_2$, 414.0794; found, 414.0781.

4.4.18. 4-((4-((4-Aminophenyl)sulfonyl)piperazin-1-yl)sulfonyl)benzene-1,2-diol (22)

Following general procedure C, **51a** (200 mg, 0.42 mmol) was reacted to afford 130 mg (69%) of 4-((4-((3,4-dimethoxyphenyl)sulfonyl)piperazin-1-yl)sulfonyl)aniline as a white solid without further purification. ^{1}H NMR (400 MHz, DMSO-d_6) δ 7.29 (t, *J* = 8.1 Hz, 3H), 7.15 (d, *J* = 8.5 Hz, 1H), 7.09 (d, *J* = 2.1 Hz, 1H), 6.65–6.61 (m, 2H), 6.12 (s, 2H), 3.85 (s, 3H), 3.82 (s, 3H), 2.97 (t, *J* = 4.9 Hz, 4H), 2.86 (d, *J* = 4.9 Hz, 4H). ^{13}C NMR (101 MHz, DMSO-d_6) δ 153.48, 152.75, 148.81, 129.56, 126.29, 121.42, 118.91, 112.75, 111.44, 109.94, 55.94, 55.88, 45.21, 45.15. Following general procedure A, 4-((4-((3,4-dimethoxyphenyl)sulfonyl)piperazin-1-yl)sulfonyl)aniline (120 mg, 0.27 mmol) was reacted to afford 40 mg (36%) of title compound as a pale-brown solid after column chromatography (DCM:MeOH 0–10%). mp: 238–240 °C. ^{1}H NMR (400 MHz, CD_3OD) δ 7.41–7.37 (m, 2H), 7.11–7.07 (m, 2H), 6.93–6.90 (m, 1H), 6.73–6.68 (m, 2H), 2.95 (s, 8H). ^{13}C NMR (101 MHz, CD_3OD) δ 154.76, 151.68, 146.87, 130.87, 126.70, 121.90, 121.73, 116.34, 115.64, 114.47, 46.77, 46.74. HRMS (*m/z*): [M]+ calcd. for $C_{16}H_{19}N_3O_6S_2$, 414.0794; found, 414.0797.

4.4.19. 6-((4-((4-Aminophenyl)sulfonyl)piperazin-1-yl)sulfonyl)-[1,1′-biphenyl]-3,3′,4,4′-tetraol (23)

Following general procedure C, **46a** (400 mg, 0.66 mmol) was reacted to afford 71 mg (19%) of 4-((4-((3′,4,4′,5-tetramethoxy-[1,1′-biphenyl]-2-yl)sulfonyl)piperazin-1-yl)sulfonyl)aniline as a pale yellow solid after column chromatography (pentane/EtOAc 50–100%). ^{1}H NMR (400 MHz, $CDCl_3$) δ 7.53 (s, 1H), 7.41 (d, *J* = 8.2 Hz, 2H), 7.03 (s, 1H), 6.83–6.78 (m, 2H), 6.74 (s, 1H), 6.68 (d, *J* = 8.2 Hz, 2H), 3.94 (s, 3H), 3.90 (d, *J* = 1.5 Hz, 6H), 3.86 (s, 3H), 2.78 (s, 8H). ^{13}C NMR (101 MHz, $CDCl_3$) δ 151.73, 148.79, 147.87, 147.58, 135.36, 131.88, 129.84, 128.06, 121.72, 115.57, 114.37, 114.16, 113.27, 110.45, 110.11, 56.48, 56.36, 56.10, 45.85, 44.18. Following general procedure A, 4-((4-((3′,4,4′,5-tetramethoxy-[1,1′-biphenyl]-2-yl)sulfonyl)piperazin-1-yl)sulfonyl)aniline (60 mg, 0.10 mmol) was reacted to afford 10 mg (19%) of title compound as a pale-brownish solid after reverse phase column chromatography (H_2O/MeOH 0–40%). mp: 163–165 °C. ^{1}H NMR (400 MHz, CD_3OD) δ 7.43 (s, 1H), 7.37–7.34 (m, 2H), 6.83 (d, *J* = 2.1 Hz, 1H), 6.76–6.72 (m, 2H), 6.65 (s, 1H), 6.59 (d, *J* = 8.1 Hz, 1H), 6.50 (dd, *J* = 8.1, 2.1 Hz, 1H), 2.80 (t, *J* = 4.9 Hz, 4H), 2.67 (t, *J* = 5.0 Hz, 4H). ^{13}C

NMR (101 MHz, CD_3OD) δ 154.69, 150.42, 145.99, 145.22, 145.03, 136.12, 132.62, 130.78, 127.35, 122.47, 122.17, 120.86, 120.83, 118.58, 118.55, 115.54, 114.63, 46.87, 45.16. HRMS (*m/z*): [M]+ calcd. for $C_{22}H_{23}N_3O_8S_2$, 522.1005; found, 522.1004.

*4.4.20. 6-((4-((3-Aminophenyl)sulfonyl)piperazin-1-yl)sulfonyl)-[1,1′-biphenyl]-3,3′,4,4′-tetraol (**24**)*

Following general procedure C, **47a** (300 mg, 0.49 mmol) was reacted to afford 230 mg (81%) of 3-((4-((3′,4,4′,5-tetramethoxy-[1,1′-biphenyl]-2-yl)sulfonyl)piperazin-1-yl)sulfonyl)aniline as a pale yellow solid after column chromatography (pentane/EtOAc 50–100%). ^{1}H NMR (400 MHz, $CDCl_3$) δ 7.54 (s, 1H), 7.27 (s, 1H), 7.04 (d, *J* = 1.2 Hz, 1H), 6.99 (dt, *J* = 7.9, 1.1 Hz, 1H), 6.93 (t, *J* = 2.0 Hz, 1H), 6.90–6.85 (m, 1H), 6.79 (d, *J* = 1.2 Hz, 2H), 6.74 (s, 1H), 3.94 (s, 3H), 3.90 (d, *J* = 1.0 Hz, 6H), 3.85 (s, 3H), 2.80 (s, 8H). ^{13}C NMR (101 MHz, $CDCl_3$) δ 151.75, 148.79, 147.89, 147.59, 136.30, 135.34, 131.90, 128.04, 121.70, 119.57, 117.42, 115.59, 115.53, 114.16, 113.31, 113.26, 110.49, 56.52, 56.46, 56.18, 56.07, 45.86, 44.20. Following general procedure A, 3-((4-((3′,4,4′,5-tetramethoxy-[1,1′-biphenyl]-2-yl)sulfonyl)piperazin-1-yl)sulfonyl)aniline (200 mg, 0.35 mmol) was reacted to afford 20 mg (11%) of title compound as a beige solid after reverse phase column chromatography (H_2O/MeOH 20–50%). mp: 200–202 °C. ^{1}H NMR (400 MHz, CD_3OD) δ 7.42 (s, 1H), 7.30 (t, *J* = 7.8 Hz, 1H), 6.98 (dd, *J* = 7.7, 2.3 Hz, 1H), 6.95 (t, *J* = 2.0 Hz, 1H), 6.91 (dd, *J* = 7.7, 1.7 Hz, 1H), 6.84 (d, *J* = 2.0 Hz, 1H), 6.64 (s, 1H), 6.54 (d, *J* = 8.1 Hz, 1H), 6.47 (dd, *J* = 8.1, 2.0 Hz, 1H), 2.81 (t, *J* = 4.8 Hz, 4H), 2.70 (t, *J* = 4.9 Hz, 4H). ^{13}C NMR (101 MHz, CD_3OD) δ 150.68, 150.38, 145.92, 145.19, 145.13, 137.33, 136.07, 132.71, 131.01, 127.05, 122.43, 120.86, 120.52, 118.57, 118.49, 117.20, 115.54, 114.09, 46.82, 45.14. HRMS (*m/z*): [M]+ calcd. for $C_{22}H_{23}N_3O_8S_2$, 522.1005; found, 522.1002.

*4.4.21. 6-((4-((3-Aminophenyl)sulfonyl)piperazin-1-yl)sulfonyl)-4′-fluoro-[1,1′-biphenyl]-3,4-diol (**25**)*

Following general procedure C, **48a** (90 mg, 0.16 mmol) was reacted to afford 76 mg (89%) of 3-((4-((4′-fluoro-4,5-dimethoxy-[1,1′-biphenyl]-2-yl)sulfonyl)piperazin-1-yl)sulfonyl)aniline as a white solid without further purification. ^{1}H NMR (400 MHz, DMSO-d_6) δ 7.40 (s, 1H), 7.30–7.25 (m, 3H), 7.03–6.98 (m, 2H), 6.89 (ddd, *J* = 8.1, 2.3, 0.9 Hz, 1H), 6.83 (d, *J* = 2.8 Hz, 2H), 6.71 (ddd, *J* = 7.7, 1.9, 0.9 Hz, 1H), 3.84 (d, *J* = 5.7 Hz, 6H), 2.77 (t, *J* = 4.9 Hz, 4H), 2.59 (t, *J* = 4.9 Hz, 4H). ^{13}C NMR (101 MHz, DMSO-d_6) δ 151.62, 149.75, 147.38, 135.01, 133.91, 131.62, 131.54, 129.83, 126.54, 118.11, 115.76, 114.19, 113.98, 112.66, 111.57, 45.18, 43.55. Following general procedure A, 3-((4-((4′-fluoro-4,5-dimethoxy-[1,1′-biphenyl]-2-yl)sulfonyl)piperazin-1-yl)sulfonyl)aniline (70 mg, 0.13 mmol) was reacted to afford 30 mg (45%) of title compound as a white-off solid after reverse phase column chromatography (H_2O/MeOH 10–70%). mp: 137–139 °C. ^{1}H NMR (400 MHz, DMSO-d_6) δ 10.12 (s, 1H), 9.82 (s, 1H), 7.37 (s, 1H), 7.27 (t, *J* = 7.9 Hz, 1H), 7.24–7.16 (m, 2H), 7.01–6.93 (m, 2H), 6.92–6.87 (m, 1H), 6.83 (t, *J* = 2.0 Hz, 1H), 6.70 (dt, *J* = 7.6, 1.3 Hz, 1H), 6.61 (s, 1H), 5.70 (s, 2H), 2.73 (t, *J* = 4.9 Hz, 4H), 2.58 (d, *J* = 4.9 Hz, 4H). ^{13}C NMR (101 MHz, DMSO-d_6) δ 161.38 (d, *J* = 244.4 Hz), 149.73, 149.32, 144.32, 135.52 (d, *J* = 3.3 Hz), 134.98, 132.32, 131.39 (d, *J* = 8.2 Hz), 129.78, 124.83, 119.77, 118.09, 117.33, 113.96, 113.93 (d, *J* = 21.3 Hz), 111.53, 45.16, 43.50. HRMS (*m/z*): [M]+ calcd. for $C_{22}H_{22}FN_3O_6S_2$, 508.1012; found, 508.1010.

*4.4.22. N-(3,4-Dihydroxyphenyl)-3,4-dihydroxybenzenesulfonamide (**26**)*

Following general procedure A, **58a** (240 mg, 0.68 mmol) was reacted to afford 50 mg (25%) of the title compound as dark-purple solid after reverse phase column chromatography (H_2O/MeOH 0–20%). mp: 191–193 °C. ^{1}H NMR (400 MHz, CD_3OD) δ 7.08–7.04 (m, 2H), 6.77 (dd, *J* = 8.3, 0.3 Hz, 1H), 6.59 (dd, *J* = 5.5, 2.9 Hz, 2H), 6.34 (dd, *J* = 8.5, 2.5 Hz, 1H). ^{13}C NMR (101 MHz, CD_3OD) δ 150.84, 146.37, 146.31, 144.32, 131.14, 130.78, 121.06, 116.16, 116.09, 115.73, 115.30, 112.53.

*4.4.23. 3,4-Dihydroxy-N-(3-hydroxyphenyl)benzenesulfonamide (**27**)*

Following general procedure A, **59a** (150 mg, 0.46 mmol) was reacted to afford 25 mg (19%) of the title compound as a grey solid after reverse phase column chromatography (H_2O/MECN 0–35%). mp: 194–196 °C. ^{1}H NMR (400 MHz, CD_3OD) δ 7.18–7.12 (m, 2H), 6.99 (t, *J* = 8.1 Hz, 1H), 6.79 (d, *J* = 8.3 Hz, 1H), 6.62 (t, *J* = 2.2 Hz, 1H), 6.50 (dddd, *J* = 16.7, 7.4, 2.2, 1.3 Hz, 2H). ^{13}C NMR (101 MHz, CD_3OD) δ 158.95, 151.00, 146.42, 140.28, 131.26, 130.68, 121.05, 115.80, 115.18, 113.20, 112.43, 109.10. HRMS (*m/z*): [M]+ calcd. for $C_{12}H_{11}NO_5S$, 282.0436; found, 282.0430.

*4.4.24. 3,4-Dihydroxy-N-phenylbenzenesulfonamide (**28**)*

Following general procedure A, **60a** (179 mg, 0.61 mmol) was reacted to afford 97 mg (60%) of the title compound as brownish solid after reverse phase column chromatography (H_2O/MeOH 0–35%). mp: 219–220 °C. ^{1}H NMR (400 MHz, CD_3OD) δ 7.22–7.14 (m, 2H), 7.13–6.99 (m, 5H), 6.74 (d, *J* = 8.3 Hz, 1H).^{13}C NMR (101 MHz, CD_3OD) δ 151.09, 146.52, 139.28, 131.26, 130.00, 125.53, 122.34, 121.04, 115.81, 115.22. HRMS (*m/z*): [M]+ calcd. for $C_{12}H_{11}NO_4S$, 266.0487; found, 266.0487.

*4.4.25. N-(3,4-Dihydroxyphenyl)-3,4-dihydroxy-N-methylbenzenesulfonamide (**29**)*

Following general procedure A, **62a** (35 mg, 0.10 mmol) was reacted to afford 13 mg (44%) of the title compound as brownish solid after reverse phase column chromatography (H_2O/MeOH 20–50%). mp: 65–67 °C. ^{1}H NMR (400 MHz, CD_3OD) δ 7.00–6.90 (m, 2H), 6.84 (dt, *J* = 8.1, 0.6 Hz, 1H), 6.68–6.63 (m, 1H), 6.56–6.47 (m, 1H), 6.37 (ddt, *J* = 8.5, 2.5, 0.7 Hz, 1H), 3.06 (d, *J* = 0.6 Hz, 3H). ^{13}C NMR (101 MHz, CD_3OD) δ 151.30, 146.42, 146.17, 146.00, 134.89, 127.85, 121.88, 119.44, 115.93, 115.81, 115.73, 115.51, 39.06. HRMS (*m/z*): [M]+ calcd. for $C_{13}H_{13}NO_6S$, 312.0542; found, 312.0543.

*4.4.26. N-(3,4-Dihydroxyphenyl)-3,4-dihydroxy-N-propylbenzenesulfonamide (**30**)*

Following general procedure A, **63a** (45 mg, 0.11 mmol) was reacted to afford 5 mg (13%) of the title compound as pale pink solid after reverse phase column chromatography (H_2O/MeOH 20–50%). mp: 85–87 °C. ^{1}H NMR (400 MHz, CD_3OD) δ 6.99–6.96 (m, 2H), 6.84 (d, *J* = 8.9 Hz, 1H), 6.66 (d, *J* = 8.4 Hz, 1H), 6.48 (d, *J* = 2.5 Hz, 1H), 6.34 (dd, *J* = 8.4, 2.5 Hz, 1H), 3.41 (t, *J* = 6.9 Hz, 2H), 1.39 (q, *J* = 7.2 Hz, 2H), 0.90 (t, *J* = 7.4 Hz, 3H). ^{13}C NMR (101 MHz, CD_3OD) δ 151.09, 146.42, 146.34, 146.28, 132.02, 129.76, 121.56, 121.46, 117.22, 115.85, 115.81, 115.70, 53.53, 22.39, 11.34. HRMS (*m/z*): [M]+ calcd. for $C_{15}H_{17}NO_6S$, 340.0855; found, 340.0858.

*4.4.27. N-(3,4-Dihydroxyphenyl)-3,4-dihydroxy-N-pentylbenzenesulfonamide (**31**)*

Following general procedure A, **64a** (50 mg, 0.12 mmol) was reacted to afford 10 mg (23%) of the title compound as brown solid after reverse phase column chromatography (H_2O/MeOH 35–70%). mp: 88–90 °C. ^{1}H NMR (400 MHz, CD_3OD) δ 7.00–6.94 (m, 2H), 6.86–6.82 (m, 1H), 6.66 (d, *J* = 8.4 Hz, 1H), 6.48 (d, *J* = 2.5 Hz, 1H), 6.34 (dd, *J* = 8.4, 2.5 Hz, 1H), 3.43 (t, *J* = 6.5 Hz, 2H), 1.40–1.25 (m, 6H), 0.91–0.82 (m, 3H). ^{13}C NMR (101 MHz, CD_3OD) δ 151.12, 146.45, 146.36, 146.31, 132.04, 129.74, 121.58, 121.47, 117.25, 115.86, 115.82, 115.72, 51.66, 29.65, 28.80, 23.22, 14.30. HRMS (*m/z*): [M]+ calcd. for $C_{17}H_{21}NO_6S$, 368.1168; found, 368.1175.

*4.4.28. N-(4-Cyanobenzyl)-3,4-dihydroxy-N-(4-hydroxy-3-(λ^1-oxidaneyl)phenyl)benzenesulfonamide (**32**)*

Following general procedure A, **67a** (80 mg, 0.17 mmol) was reacted to afford 18 mg (26%) of the title compound as a grey solid after reverse phase column chromatography (H_2O/MeOH 0–35%). mp: 83–85 °C. ^{1}H NMR (400 MHz, CD_3OD) δ 7.60 (d, *J* = 8.0 Hz, 2H), 7.44 (d, *J* = 8.0 Hz, 2H), 7.12–7.02 (m, 2H), 6.88 (d, *J* = 8.3 Hz, 1H), 6.57 (d, *J* = 8.4 Hz,

1H), 6.47–6.42 (m, 1H), 6.31 (dd, $J = 8.5$, 2.5 Hz, 1H), 4.71 (s, 2H). ^{13}C NMR (101 MHz, CD_3OD) δ 151.45, 146.62, 146.46, 146.28, 144.17, 133.18, 131.89, 130.42, 129.54, 121.72, 121.48, 119.59, 117.36, 116.05, 115.81, 115.76, 112.20, 55.57. HRMS (*m/z*): [M]+ calcd. for $C_{20}H_{16}N_2O_6S$, 413.0807; found, 413.0804.

4.4.29. N-(4-Fluorophenyl)-3,4-dihydroxy-N-methylbenzenesulfonamide (33)

Following general procedure A, **65a** (70 mg, 0.22 mmol) was reacted to afford 40 mg (63%) of the title compound as a pale beige solid after reverse phase column chromatography (H_2O/MeOH 0–35%). mp: 90–93 °C. ^{1}H NMR (400 MHz, CD_3OD) δ 7.12–7.08 (m, 2H), 7.06–7.01 (m, 2H), 6.93–6.90 (m, 1H), 6.88 (t, $J = 1.6$ Hz, 1H), 6.84 (dd, $J = 8.3$, 0.9 Hz, 1H), 3.11 (d, $J = 1.0$ Hz, 3H). ^{13}C NMR (101 MHz, CD_3OD) δ 162.87 (d, $J = 245.6$ Hz), 151.52, 146.54, 139.31 (d, $J = 3.1$ Hz), 129.83 (d, $J = 8.6$ Hz), 127.37, 121.85, 116.39 (d, $J = 22.9$ Hz), 115.92, 115.78, 38.70.

4.4.30. N-(4-Fluorophenyl)-3,4-dihydroxy-N-propylbenzenesulfonamide (34)

Following general procedure A, **66a** (70 mg, 0.20 mmol) was reacted to afford 30 mg (47%) of the title compound as a white solid after reverse phase column chromatography (H_2O/MeOH 0–35%). mp: 139–140 °C. ^{1}H NMR (400 MHz, CD_3OD) δ 7.06 (d, $J = 6.6$ Hz, 4H), 6.96–6.92 (m, 2H), 6.86–6.82 (m, 1H), 3.48 (t, $J = 6.9$ Hz, 2H), 1.38 (m, 2H), 0.90 (t, $J = 7.4$ Hz, 3H). ^{13}C NMR (101 MHz, CD_3OD) δ 163.24 (d, $J = 246.4$ Hz), 151.37, 146.60, 136.76 (d, $J = 3.0$ Hz), 131.96 (d, $J = 8.8$ Hz), 129.29, 121.56, 116.57 (d, $J = 22.9$ Hz), 115.97, 115.60, 53.30, 22.41, 11.28. HRMS (*m/z*): [M]+ calcd. for $C_{15}H_{16}FNO_4S$, 326.0862; found, 326.0863.

4.4.31. N-(3,4-Dihydroxyphenyl)-3′,4,4′,5-tetrahydroxy-[1,1′-biphenyl]-2-sulfonamide (35)

Following general procedure A, **71a** (420 mg, 0.86 mmol) was reacted to afford 143 mg (41%) of the title compound as pale-brownish solid after reverse phase column chromatography (H_2O/MECN 0–15%). ^{1}H NMR (400 MHz, CD_3OD) δ 7.41 (s, 1H), 6.78–6.75 (m, 2H), 6.62–6.59 (m, 2H), 6.55 (d, $J = 8.5$ Hz, 1H), 6.44 (d, $J = 2.5$ Hz, 1H), 6.18 (dd, $J = 8.5$, 2.6 Hz, 1H). ^{13}C NMR (101 MHz, CD_3OD) δ 149.93, 146.35, 146.00, 145.22, 144.85, 143.42, 135.78, 132.45, 130.77, 129.34, 122.65, 120.43, 118.41, 118.17, 116.11, 115.50, 113.88, 110.39. Data matches according with previous report [26].

4.4.32. 3′,4,4′,5-Tetrahydroxy-N-phenyl-[1,1′-biphenyl]-2-sulfonamide (36)

Following general procedure A, **71a** (86 mg, 0.20 mmol) was reacted to afford 22 mg (29%) of the title compound as beige solid after reverse phase column chromatography (H_2O/MECN 0–15%). ^{1}H NMR (400 MHz, CD_3OD) δ 7.52 (s, 1H), 7.13 (t, $J = 8.0$ Hz, 2H), 6.93 (t, $J = 7.4$ Hz, 1H), 6.80 (d, $J = 7.5$ Hz, 2H), 6.75 (d, $J = 8.1$ Hz, 1H), 6.68 (s, 1H), 6.57 (s, 1H), 6.53 (d, $J = 8.2$ Hz, 1H). ^{13}C NMR (101 MHz, CD_3OD) δ 148.74, 144.67, 143.86, 143.56, 137.47, 134.49, 130.82, 128.36, 127.69, 122.79, 121.10, 119.04, 118.35, 116.89, 116.84, 114.10. Data matches according with previous report [26].

4.4.33. N-(3,4-Dihydroxyphenyl)-3′,4,4′,5-tetrahydroxy-N-methyl-[1,1′-biphenyl]-2-sulfonamide (37)

Following general procedure A, **72a** (74 mg, 0.15 mmol) was reacted to afford 9 mg (15%) of the title compound as brownish solid after reverse phase column chromatography (H_2O/MeOH 0–30%). mp: 150–152 °C. ^{1}H NMR (400 MHz, CD_3OD) δ 7.23 (s, 1H), 6.82 (d, $J = 2.1$ Hz, 1H), 6.72 (d, $J = 8.1$ Hz, 1H), 6.64 (s, 1H), 6.62 (dd, $J = 8.1$, 2.1 Hz, 1H), 6.57 (d, $J = 8.5$ Hz, 1H), 6.49 (d, $J = 2.5$ Hz, 1H), 6.25 (dd, $J = 8.5$, 2.6 Hz, 1H), 2.68 (s, 3H). ^{13}C NMR (101 MHz, CD_3OD) δ 150.01, 146.26, 145.87, 145.70, 145.11, 144.70, 136.27, 134.39, 132.90, 128.91, 123.09, 120.78, 119.73, 118.97, 118.72, 115.88, 115.58, 115.27, 39.20. HRMS (*m/z*): [M]+ calcd. for $C_{19}H_{17}NO_8S$, 420.0753; found, 420.0751.

4.4.34. N,N′-(Ethane-1,2-diyl)bis (3′,4,4′,5-tetrahydroxy-N-methyl-[1,1′-biphenyl]-2-sulfonamide) (38)

Following general procedure A, **74a** (75 mg, 0.099 mmol) was reacted to afford 13 mg (20%) of the title compound as beige solid after reverse phase column chromatography (H_2O/MeOH 25–60%). mp: 220–222 °C. ^{1}H NMR (400 MHz, CD_3OD) δ 7.41 (s, 1H), 6.78–6.73 (m, 2H), 6.64 (s, 1H), 6.59 (dd, $J = 8.1$, 2.1 Hz, 1H), 2.47 (s, 2H), 2.29 (s, 3H). ^{13}C NMR (101 MHz, CD_3OD) δ 149.92, 145.98, 145.23, 144.89, 135.73, 132.57, 128.65, 122.64, 120.71, 118.55, 118.52, 115.50, 48.28, 34.29. HRMS (*m/z*): [M]+ calcd. for $C_{28}H_{28}N_2O_{12}S_2$, 649.1162; found, 649.1181.

4.4.35. N-(3-(4-(((4-Aminophenyl)sulfonamido)methyl)benzyl)phenyl) acetamide (39)

Following general procedure C, **84a** (260 mg, 0.59 mmol) was reacted to afford 210 mg (87%) of the title compound as a white solid after reverse phase column chromatography (H_2O/MeOH 50–100%). mp: 209–211 °C. ^{1}H NMR (400 MHz, Acetone-d_6) δ 9.06 (s, 1H), 7.64–7.46 (m, 4H), 7.23–7.06 (m, 6H), 6.72 (dd, $J = 8.6$, 1.7 Hz, 2H), 6.41 (t, $J = 6.4$ Hz, 1H), 5.42 (s, 2H), 3.99 (d, $J = 6.5$ Hz, 2H), 3.89 (s, 2H), 2.82 (s, 3H). ^{13}C NMR (101 MHz, DMSO-d_6) δ 168.04, 152.44, 140.30, 137.30, 135.83, 135.54, 128.80, 128.46, 128.43, 127.70, 125.54, 119.13, 112.65, 45.87, 40.15, 23.92. HRMS (*m/z*): [M]+ calcd. for $C_{22}H_{23}N_3O_3S$, 410.1538; found, 410.1539.

4.4.36. 4-Amino-N-(4-(3-aminobenzyl)benzyl)benzenesulfonamide (40)

Compound **39** (20 mg, 0.05 mmol) was suspended with HCl in 1,4-dioxane (2 mL), the mixture was heated to reflux until complete hydrolysis of acetyl group approximately 2 h. The mixture was cooled down to room temperature, and the solution was neutralized with NaOH 1 M, the white suspension was extracted with ethyl acetate, and washed with brine. The organic phase was dried over sodium sulphate and the solvent was filtered and the solvent was evaporated to afford 13 mg (72%) as a brownish solid after column chromatography (DCM/MeOH 10%). mp: 118–120 °C. ^{1}H NMR (400 MHz, CD_3OD) δ 7.96 (d, $J = 8.1$ Hz, 2H), 7.54 (d, $J = 8.1$ Hz, 2H), 7.34 (q, $J = 8.3$ Hz, 4H), 7.14 (q, $J = 7.9$ Hz, 4H), 4.05 (s, 2H), 3.99 (s, 2H). ^{13}C NMR (101 MHz, CD_3OD) δ 144.21, 141.21, 138.06, 136.67, 131.54, 130.01, 129.99, 129.78, 129.22, 124.13, 123.78, 47.54, 41.68. HRMS (*m/z*): [M]+ calcd. for $C_{20}H_{21}N_3O_2S$, 368.1433; found, 368.1430.

4.4.37. N-(4-(3,4-Dihydroxybenzyl)benzyl)-3,4-dihydroxybenzenesulfonamide (41)

Following general procedure A, **85a** (80 mg, 0.17 mmol) was reacted to afford 15 mg (21%) of the title compound as a white solid after reverse phase column chromatography (SNAP C18 30 g, 20–80% MeOH/H_2O). mp: 78.79 °C. ^{1}H NMR (400 MHz, CD_3OD) δ 7.24–7.17 (m, 2H), 7.14–7.02 (m, 4H), 6.85 (d, $J = 8.3$ Hz, 1H), 6.65 (d, $J = 8.0$ Hz, 1H), 6.55 (d, $J = 1.9$ Hz, 1H), 6.47 (dd, $J = 8.0$, 2.0 Hz, 1H), 3.95 (s, 2H), 3.75 (s, 2H). ^{13}C NMR (101 MHz, CD_3OD) δ 149.42, 145.26, 144.73, 143.04, 141.19, 134.76, 132.82, 130.65, 128.41, 127.54, 119.75, 119.37, 115.61, 114.82, 114.62, 113.67, 46.32, 40.37. HRMS (*m/z*): [M+H] calcd. for $C_{20}H_{19}NO_6S$, 402.101; found, 402.102.

4.4.38. N-(4-(3,4-Dihydroxybenzyl)benzyl)benzenesulfonamide (42)

Following general procedure A, **86a** (150 mg, 0.38 mmol) was reacted to afford 101 mg (72%) of the title compound as a white solid after reverse phase column chromatography (SNAP C18 30 g, 20–100% MeCN/H_2O). mp: 144–146 °C. ^{1}H NMR (400 MHz, CD_3OD) δ 7.79–7.74 (m, 2H), 7.56–7.50 (m, 1H), 7.48–7.41 (m, 2H), 7.09–7.00 (m, 4H), 6.66 (d, $J = 8.0$ Hz, 1H), 6.55 (d, $J = 2.1$ Hz, 1H), 6.47 (dd, $J = 8.0$, 2.1 Hz, 1H), 4.01 (s, 2H), 3.72 (s, 2H). ^{13}C NMR (101 MHz, CD_3OD) δ 144.78, 143.08, 141.27, 140.76, 134.52, 132.82, 132.01, 128.63, 128.37, 127.54, 126.49, 119.67, 115.60, 114.77, 46.29, 40.41. HRMS (*m/z*): [M

− H] calcd. for $C_{20}H_{18}NO_4S$, 345.106; found, 345.106.

4.4.39. N-(4-(3,4-Dihydroxybenzyl)benzyl)naphthalene-2-sulfonamide (43)

Following general procedure A, **87a** (168 mg, 0.38 mmol) was reacted to afford 141 mg (90%) of the title compound as a white solid after reverse phase column chromatography (SNAP C18 30 g, 20–100% MeCN/H_2O). mp: 130–133 °C. ^{1}H NMR (400 MHz, CD_3OD) δ 8.31 (s, 1H), 7.98–7.88 (m, 3H), 7.73 (d, J = 8.7 Hz, 1H), 7.62 (p, J = 6.9 Hz, 2H), 7.03 (d, J = 7.9 Hz, 2H), 6.92 (d, J = 7.9 Hz, 2H), 6.64 (d, J = 8.0 Hz, 1H), 6.52 (s, 1H), 6.39 (d, J = 8.0 Hz, 1H), 4.04 (s, 2H), 3.62 (s, 2H). ^{13}C NMR (101 MHz, CD_3OD) δ 144.75, 143.05, 141.22, 137.67, 134.63, 134.41, 132.71, 132.11, 128.92, 128.74, 128.30, 128.27, 127.65, 127.58, 127.54, 127.11, 121.97, 119.69, 115.60, 114.80, 46.37, 40.30. HRMS (*m/z*): [M+H] calcd. for $C_{24}H_{21}NO_4S$, 420.127; found, 420.127.

4.4.40. N-(4-(3,4-Dihydroxybenzyl)benzyl)-3′,4,4′,5-tetrahydroxy-[1,1′-biphenyl]-2-sulfonamide (44)

Following general procedure A, **88a** (125 mg, 0.21 mmol) was reacted to afford 10 mg (9%) of the title compound as a translucent solid after reverse phase column chromatography (SNAP C18 30 g, 20–100% MeCN/H_2O). mp: 142–144 °C. ^{1}H NMR (400 MHz, CD_3OD) δ 7.46 (s, 1H), 7.06–6.96 (m, 4H), 6.86 (d, J = 2.0 Hz, 1H), 6.72 (d, J = 8.1 Hz, 1H), 6.69–6.63 (m, 3H), 6.54 (d, J = 1.8 Hz, 1H), 6.47 (dd, J = 8.6, 1.3 Hz, 1H), 3.74 (s, 2H), 3.71 (s, 2H). ^{13}C NMR (101 MHz, CD_3OD) δ 148.62, 144.93, 144.73, 144.28, 143.83, 143.05, 141.31, 134.31, 133.46, 132.76, 130.66, 128.44, 120.85, 119.75, 118.80, 116.74, 115.90, 115.60, 114.82, 114.37, 46.34, 40.35. HRMS (*m/z*): [M+H] calcd. for $C_{26}H_{23}NO_8S$, 510.122; found, 510.122.

4.4.41. N-(4-(3,4-Dihydroxybenzyl)benzyl)-3′,4′-dihydroxy-[1,1′-biphenyl]-2-sulfonamide (45)

Following general procedure A, **89a** (80 mg, 0.15 mmol) was reacted to afford 65 mg (91%) of the title compound as a white solid after reverse phase column chromatography (SNAP C18 30 g, 30–100% MeCN/H_2O). mp: 79–82 °C. ^{1}H NMR (400 MHz, CD_3OD) δ 8.00 (d, J = 8.0 Hz, 1H), 7.55 (t, J = 7.5 Hz, 1H), 7.43 (t, J = 7.7 Hz, 1H), 7.27 (d, J = 7.6 Hz, 1H), 7.06–6.93 (m, 4H), 6.87 (d, J = 2.1 Hz, 1H), 6.76 (d, J = 8.1 Hz, 1H), 6.69–6.60 (m, 2H), 6.55 (d, J = 1.9 Hz, 1H), 6.47 (dd, J = 8.0, 2.0 Hz, 1H), 3.77 (s, 2H), 3.73 (s, 2H). ^{13}C NMR (101 MHz, CD_3OD) δ 145.24, 144.77, 144.36, 143.07, 141.38, 140.92, 138.65, 134.25, 132.80, 132.56, 131.83, 130.56, 128.43, 128.41, 127.71, 126.95, 120.84, 119.72, 116.64, 115.61, 114.81, 114.45, 46.31, 40.39. HRMS (*m/z*): [M+H] calcd. for $C_{26}H_{23}NO_6S$, 478.132; found, 478.132.

4.4.42. N-(4-(3,4-Dihydroxybenzyl)benzyl)-4′-fluoro-4,5-dihydroxy-[1,1′-biphenyl]-2-sulfonamide (46)

Following general procedure A, **92a** (190 mg, 0.34 mmol) was reacted to afford 15 mg (9%) of the title compound as a translucent solid after reverse phase column chromatography (SNAP C18 30 g, 20–100% MeCN/H_2O). mp: 121–124 °C. ^{1}H NMR (400 MHz, CD_3OD) δ 7.49 (s, 1H), 7.19 (dd, J = 8.4, 5.5 Hz, 2H), 7.04 (d, J = 7.7 Hz, 2H), 7.02–6.92 (m, 4H), 6.69–6.60 (m, 2H), 6.57 (s, 1H), 6.48 (d, J = 8.0 Hz, 1H), 3.81 (s, 2H), 3.74 (s, 2H). ^{13}C NMR (101 MHz, CD_3OD) δ 162.25 (d, J = 245.0 Hz), 148.51, 144.73, 144.09, 143.04, 141.36, 135.45 (d, J = 3.4 Hz), 134.62, 132.87, 132.63, 131.30 (d, J = 8.1 Hz), 129.07, 128.34, 127.70, 119.71, 118.94, 116.17, 115.57, 114.83, 113.85 (d, J = 21.6 Hz), 45.99, 40.39. HRMS (*m/z*): [M + H + Na] calcd. for $C_{26}H_{21}FNO_6SNa$, 495.115; found, 495.115.

4.4.43. N-(4-(3,4-Dihydroxybenzyl)benzyl)-4′-fluoro-[1,1′-biphenyl]-2-sulfonamide (47)

Following general procedure A, **93a** (300 mg, 0.61 mmol) was reacted to afford 214 mg (76%) of the title compound as a white solid after reverse phase column chromatography (SNAP C18 30 g, 30–100% MeCN/H_2O). mp: 55–58 °C. ^{1}H NMR (400 MHz, CD_3OD) δ 7.99 (dd, J = 8.0, 1.3 Hz, 1H), 7.54 (td, J = 7.5, 1.4 Hz, 1H), 7.48–7.41 (m, 1H), 7.25–7.10 (m, 3H), 7.07–6.96 (m, 4H), 6.90 (d, J = 8.2 Hz, 2H), 6.65 (d, J = 8.0 Hz, 1H), 6.56 (d, J = 2.0 Hz, 1H), 6.47 (dd, J = 8.0, 2.1 Hz, 1H), 3.87 (s, 2H), 3.71 (s, 2H). ^{13}C NMR (101 MHz, Acetone-d_6) δ 162.42 (d, J = 244.9 Hz), 144.96, 143.25, 141.38, 139.80 (d, J = 12.0 Hz), 134.91, 133.06, 132.75, 131.99, 131.48 (d, J = 8.2 Hz), 128.87, 128.54, 127.99, 127.82, 119.94, 115.80, 115.06, 114.35 (d, J = 21.7 Hz), 46.31, 40.52. HRMS (*m/z*): [M+H] calcd. for $C_{26}H_{22}FNO_4S$, 464.133; found, 464.132.

4.4.44. N-(4-(3,4-Dihydroxybenzyl)benzyl)-4′-fluoro-N-methyl-[1,1′-biphenyl]-2-sulfonamide (48)

Following general procedure A, **94a** (17 mg, 0.03 mmol) was reacted to afford 10 mg (62%) of the title compound as a white solid after reverse phase column chromatography (SNAP C18 30 g, 20–100% MeCN/H_2O). mp: 51–55 °C. ^{1}H NMR (400 MHz, Acetone-d_6) δ 8.10 (dd, J = 7.9, 1.4 Hz, 1H), 7.74–7.63 (m, 3H), 7.63–7.56 (m, 1H), 7.44–7.32 (m, 3H), 7.22–7.02 (m, 6H), 6.71 (d, J = 8.0 Hz, 1H), 6.64 (d, J = 2.0 Hz, 1H), 6.53 (dd, J = 8.0, 2.1 Hz, 1H), 3.79 (d, J = 9.6 Hz, 4H), 2.31 (s, 3H). ^{13}C NMR (101 MHz, Acetone-d_6) δ 162.44 (d, J = 245.0 Hz), 144.91, 143.25, 141.62, 140.37, 138.62, 135.91 (d, J = 3.4 Hz), 133.82, 133.14, 132.92, 132.26, 131.78 (d, J = 8.3 Hz), 129.74, 128.77, 128.19, 127.96, 119.99, 115.79, 115.08, 114.21 (d, J = 21.6 Hz), 52.28, 40.50, 32.60. HRMS (*m/z*): [M+H] calcd. for $C_{27}H_{24}FNO_4S$, 478.149; found, 478.149.

4.4.45. 2′-(N-(4-(3,4-Dihydroxybenzyl)benzyl)sulfamoyl)-4′,5′-dihydroxy-[1,1′-biphenyl]-4-carboxamide (49)

Following general procedure A, **95a** (51 mg, 0.09 mmol) was reacted to afford 8 mg (17%) of the title compound as a white solid after reverse phase column chromatography (SNAP C18 30 g, 20–100% MeCN/H_2O). mp: 116–120 °C. ^{1}H NMR (400 MHz, CD_3OD) δ 7.76 (dd, J = 8.1, 1.4 Hz, 2H), 7.47 (d, J = 1.5 Hz, 1H), 7.29 (dd, J = 8.1, 1.4 Hz, 2H), 7.06–6.91 (m, 4H), 6.64 (dd, J = 8.0, 1.4 Hz, 1H), 6.60 (d, J = 1.4 Hz, 1H), 6.57–6.52 (m, 1H), 6.48–6.44 (m, 1H), 3.81 (s, 2H), 3.73 (s, 2H). ^{13}C NMR (101 MHz, CD_3OD) δ 170.76, 148.62, 144.72, 144.37, 143.38, 143.05, 141.32, 134.62, 132.85, 132.65, 132.33, 129.62, 128.99, 128.35, 127.68, 126.46, 119.73, 118.57, 116.23, 115.58, 114.84, 48.00, 45.96, 40.38. HRMS (*m/z*): [M+H] calcd. for $C_{27}H_{24}N_2O_7S$, 521.138; found, 521.138.

4.4.46. N-(4-(3,4-dihydroxybenzyl)benzyl)-4,5-dihydroxy-[1,1′-biphenyl]-2-sulfonamide (50)

Following general procedure A, **96a** (46 mg, 0.09 mmol) was reacted to afford 18 mg (44%) of the title compound as a translucent solid after reverse phase column chromatography (SNAP C18 30 g, 20–100% MeCN/H_2O). mp: 123–126 °C. ^{1}H NMR (400 MHz, CD_3OD) δ 7.48 (s, 1H), 7.28–7.24 (m, 5H), 7.03–6.93 (m, 4H), 6.64 (t, J = 4.0 Hz, 2H), 6.54 (d, J = 2.1 Hz, 1H), 6.46 (dd, J = 8.0, 2.1 Hz, 1H), 3.73 (d, J = 5.1 Hz, 4H). ^{13}C NMR (101 MHz, CD_3OD) δ 148.54, 144.74, 144.02, 143.04, 141.34, 139.39, 134.51, 133.57, 132.82, 129.39, 128.71, 128.36, 127.63, 127.29, 127.19, 119.70, 118.77, 116.06, 115.57, 114.81, 46.08, 40.37.

4.4.47. Methyl 2′-(N-(4-(3,4-dihydroxybenzyl)benzyl)sulfamoyl)-4′,5′-dihydroxy-[1,1′-biphenyl]-4-carboxylate (51)

Following general procedure A, **97a** (133 mg, 0.23 mmol) was reacted to afford 11 mg (9%) of the title compound as a white solid after reverse phase column chromatography (SNAP C18 30 g, 10–80% MeOH/H_2O). mp: 96–99 °C. ^{1}H NMR (400 MHz, CD_3OD) δ 7.90 (d, J = 8.2 Hz, 2H), 7.47 (s, 1H), 7.29 (d, J = 8.2 Hz, 2H), 7.04–6.92 (m, 4H), 6.66–6.59 (m, 2H), 6.55 (d, J = 1.9 Hz, 1H), 6.46 (dd, J = 8.0, 1.9 Hz, 1H), 3.89 (s, 3H), 3.82 (s, 2H), 3.73 (s, 2H). ^{13}C NMR (101 MHz, CD_3OD) δ 167.05, 148.55, 144.74, 144.71, 144.41, 143.05, 141.33, 134.64, 132.81, 132.55, 129.66, 129.05, 128.73, 128.33, 128.26, 127.68, 119.69, 118.44, 116.23, 115.56, 114.81, 51.20, 46.91, 40.38. HRMS (*m/z*): [M − H] calcd. for $C_{28}H_{25}NO_8S$, 534.122; found, 534.123.

4.4.48. 2'-(N-(4-(3,4-dihydroxybenzyl)benzyl)sulfamoyl)-[1,1'-biphenyl]-4-carboxamide (52)

Following general procedure A, **98a** (38 mg, 0.07 mmol) was reacted to afford 16 mg (45%) of the title compound as a white solid after reverse phase column chromatography (SNAP C18 30 g, 20–100% MeOH/H_2O). ^{1}H NMR (400 MHz, CD_3OD) δ 7.99 (d, J = 7.9 Hz, 1H), 7.81 (d, J = 8.2 Hz, 2H), 7.58–7.52 (m, 1H), 7.45 (td, J = 7.8, 1.2 Hz, 1H), 7.28 (d, J = 8.2 Hz, 2H), 7.18 (d, J = 7.5 Hz, 1H), 7.01–6.88 (m, 4H), 6.65 (d, J = 8.0 Hz, 1H), 6.56 (d, J = 2.0 Hz, 1H), 6.46 (dd, J = 8.0, 1.9 Hz, 1H), 3.87 (s, 2H), 3.70 (s, 2H). ^{13}C NMR (101 MHz, CD_3OD) δ 170.67, 144.79, 143.13, 143.07, 141.43, 140.08, 139.21, 134.48, 132.92, 132.71, 132.19, 131.84, 128.54, 128.33, 127.78, 127.75, 126.55, 119.70, 115.61, 114.84, 46.05, 40.44. HRMS (m/z): [M+H] calcd. for $C_{27}H_{24}N_2O_5S$, 489.148; found, 489.148.

4.5. Determination of PKL activity after treatment of cell lysates with the compounds

HepG2 PKM2 KO, a human liver cell line containing mostly the PKL isoform, was obtained from Synthego (CA, USA). Cells were maintained in a growing medium (RPMI 1640 medium supplemented with 2 mM glutamine and 10% FBS). Twenty-four hours before the experiment, cells were plated in 10 cm dishes (3.6 × 10^5 cells/dish). Cells were washed three times with PBS and lysed thereafter on ice with 720 μl/dish of PK assay buffer (Abcam). The cell lysate was centrifuged for 10 min at 14 000×g to remove the cellular debris. The protein concentration of the cell lysate was determined using a BCA kit (Pierce) and adjusted to 200 μg/mL. The cell lysates (10 μg total protein) were incubated in triplicates for 5 min at RT with 10 μM compounds or vehicle (DMSO). PKL activity was determined using a kit from Abcam according to the manufacturer's instructions. The PKL activity in the cell lysates treated with the compounds was expressed as a percentage of the PK activity in the vehicle.

4.6. Determination of PKL activity after treatment of cells with the compounds

One day before the experiment, the HepG2 PKM2 KO cells were plated in 6 well plates (10^5-3x10^5 cells/well) and treated in triplicates for 4 and 48 h with 10 μM compounds or DMSO in the growing medium. Cells were washed 3 times with PBS and lysed with 200 μl/well PK assay buffer. The cell lysates were centrifuged for 10 min at 14 000×g to remove the cellular debris. The protein concentration of the cell lysates was determined using a BCA kit (Pierce) and adjusted to 200 μg/mL. PKL activity was determined with 10 μg total protein/reaction using a kit from Abcam according to the manufacturer's instructions. The PKL activity of compounds-treated cells was expressed as a percentage of the PK activity in vehicle-treated cells.

4.7. ADP-Glo assay to determine AC_{50} or IC_{50}

Pyruvate kinase liver reactions were conducted in triplicates at room temperature for 30 min in a 5 μl mixture containing 50 mM Tris, pH 7.4, 10 mM $MgCl_2$, 100 mM KCl, 0.05% Tween, 1.0 mM ADP, 0.3 mM PEP, pyruvate kinase (0.3 ng/μl) and the test compounds at a range of concentration 25–0.049 μM. The final DMSO in the reaction is 1%. After enzymatic reactions, 5 μl of Kinase-Glo Max reagent was added to each well and luminescence was measured using a SpectraMax iD5 microplate reader. The Kinase-Glo Max luminescence assay kit measures PK activity by quantitating the amount of ATP produced following a PK reaction. The values of % activity versus a series of compound concentrations were plotted using non-linear regression analysis of the Sigmoidal dose-response curve generated with equation Y=B+(T-B)/1 + $10^{((\mathrm{LogEC50}-X)\times \mathrm{Hill\ Slope})}$, where Y = percent activity, B = minimum percentage activity, T = maximum percentage activity, X = logarithm of compound and Hill Slope = slope factor or Hill coefficient. The EC_{50} or IC_{50} value was determined by the concentration causing a half-maximal percentage activity.

4.8. Crystallography

Human PKL expression cassette in a T7 promoter-based pExp-NHis vector (Addgene plasmid #112558) contained a S12D phosphomimic mutation and an internal deletion of the B-domain (aa 130–230, replaced by Gly-Ser-Gly linker) in PKL coding region, preceded by an *N*-terminal fusion of 8 × His-tag and a TEV protease cleavage site. The protein was produced in T7 Express cells (NEB) cultured in 2xYT media with overnight expression at 18 °C induced with 0.4 mM IPTG. The protein was purified first by immobilized metal affinity chromatography using PureCube Ni-NTA resin (Cube Biotech) and then N-terminal His-tag was removed by the cleavage with TEV protease (produced in-house). The protein was further purified by anion-exchange chromatography using HiTrap Q HP 5 mL column (Cytiva) and, finally, by size exclusion chromatography using a Superdex 200 16/600 column (Cytiva). Protein solution in 20 mM HEPES-NaOH pH 7.2, 200 mM NaCl, 50 mM KCl, 5% glycerol, 0.5 mM TCEP was concentrated to 7.5 mg/mL, supplemented with 1 mM fructose 1,6-bisphosphate (FBP), aliquoted and flash-frozen in liquid nitrogen.

PKL was crystalised by mixing equal volumes (250 nl) of protein solution with crystallisation conditions containing 100 mM HEPES-MOPS pH7.5, 10% PEG 8000, 20% EG, 10 mM phenylalanine, 20 mM sodium oxalate. Crystals usually appeared already after 12 h. For soaking, 1 mM (final) compound was added to the drop with crystals for 12–24 h, after which they were cryo-cooled in liquid nitrogen for data collection. Data were collected at Diamond Light Source, typically 180° of data with 0.1° oscillation per image. The was processed at Diamond automatically with autoPROC and Staraniso packages, and final datasets were typically around 2.0 Å in resolution. The structures were determined using a pipedream package (Global Phasing) and refined with Buster. Mogul (CCDC) was used for the generation of ligand restraints. The structures contain two PKL tetramers in the asymmetric unit, with each protomer bound to FBP and oxalate coordinating the active site Mg^{2+}. The eight active sites in the asymmetric unit had different accessibility for ligands, and typically good electron density was found for 4–6 inhibitors only. Data collection and refinement statistics are shown in Supplementary Table S3. All structures have been deposited in the Protein Data Bank under the following deposition codes (ligand number in parenthesis after each code): 7FRV (**3**), 7FRW (**4**), 7FRX (**5**), 7FRY (**6**), 7FRZ (**7**), 7FS0 (**8**), 7FS1 (**11**), 7FS2 (**13**), 7FS3 (**15**), 7FS4 (**16**), 7FS5 (**17**), 7FS6 (**18**), 7FS7 (**20**), 7FS8 (**21**), 7FS9 (**22**), 7FSA (**24**), 7FSB (**41**), 7FSC (**42**), 7FSD (**44**).

4.9. Molecular modelling

Molecular modelling studies were conducted using Molecular Operating Environment (MOE) [27] version MOE 2019.0102 (Chemical Computing Group, Montreal, CA). The X-ray crystallographic complexes were prepared based on the chain A & C of the protein using the MOE quick preparation tool. We used as parameters a forcefield: Amber 10: EHT and solvation: R-Field. Each compound data was prepared by minimising energy, adding hydrogen atoms, and calculating partial charges and potential energy. Dockings were carried out as a triangle matcher, induced fit, score London dG and 30 poses, and refinement of returned 5 poses for each compound. Validation was achieved by restoring the original orientation upon redocking.

Declaration of competing interest

The authors declare that they have no known competing financial interests or personal relationships that could have appeared to influence the work reported in this paper.

Data availability

Data will be made available on request.

Acknowledgments

The authors acknowledge financial support from the Swedish Research Council (Grant #: 2019–01049 to JB), the NovoNordisk Foundation (Grant #: 0063869 to JB) and from the Torsten Söderberg Foundation (Grant #: M105/19 to JB). We are grateful to the Diamond Light Source for access to beamlines I03, I04 and I04-1 and for the data contributing to these results (proposals mx18548 and mx25402). We thank the X-ray crystallographic facility at the Department of Biochemistry, Cambridge, for access to crystallisation instrumentation.

Appendix A. Supplementary data

Supplementary data to this article can be found online at https://doi.org/10.1016/j.ejmech.2023.115177.

References

[1] A. Kumari, Glycolysis, Academic Press, 2018, https://doi.org/10.1016/B978-0-12-814453-4.00001-7.
[2] L.A. Fothergill-Gilmore, P.A.M. Michels, Evolution of glycolysis, Prog. Biophys. Mol. Biol. 59 (1993) 105–235, https://doi.org/10.1016/0079-6107(93)90001-Z.
[3] P.A.O. Weernink, G.E.J. Stoal, G. Rijksen, Pyruvate kinases, in: Encyclopedia of Cancer, second ed., Academic Press, 2002, pp. 535–547, https://doi.org/10.1016/B0-12-227555-1/00518-9.
[4] G. Valentini, L. Chiarelli, R. Fortini, M.L. Speranza, A. Galizzi, A. Mattevi, The allosteric regulation of pyruvate kinase: a site-directed mutagenesis study, J. Biol. Chem. 275 (2000) 18145–18152, https://doi.org/10.1074/jbc.M001870200.
[5] A. Mattevi, M. Bolognesi, G. Valentini, The allosteric regulation of pyruvate kinase, FEBS Lett. 389 (1996) 15–19, https://doi.org/10.1016/0014-5793(96)00462-0.
[6] E.R. Wall, G.L. Cottam, Isozymes of pyruvate kinase in vertebrates: their physical, chemical, kinetic and immunological properties, Int. J. Biochem. 9 (1978) 785–794, https://doi.org/10.1016/0020-711X(78)90027-7.
[7] Z. Liu, C. Zhang, S. Lee, W. Kim, M. Klevstig, A.M. Harzandi, N. Sikanic, M. Arif, M. Ståhlman, J. Nielsen, M. Uhlen, J. Boren, A. Mardinoglu, Pyruvate kinase L/R is a regulator of lipid metabolism and mitochondrial function, Metab. Eng. 52 (2019) 263–272, https://doi.org/10.1016/j.ymben.2019.01.001.
[8] S. Lee, C. Zhang, Z. Liu, M. Klevstig, B. Mukhopadhyay, M. Bergentall, R. Cinar, M. Ståhlman, N. Sikanic, J.K. Park, S. Deshmukh, A.M. Harzandi, T. Kuijpers, M. Grøtli, S.J. Elsässer, B.D. Piening, M. Snyder, U. Smith, J. Nielsen, F. Bäckhed, G. Kunos, M. Uhlen, J. Boren, A. Mardinoglu, Network analyses identify liver-specific targets for treating liver diseases, Mol. Syst. Biol. 13 (2017) 938, https://doi.org/10.15252/msb.20177703.
[9] K. Chella Krishnan, R.R. Floyd, S. Sabir, D.W. Jayasekera, P.v. Leon-Mimila, A. E. Jones, A.A. Cortez, V. Shravah, M. Péterfy, L. Stiles, S. Canizales-Quinteros, A. S. Divakaruni, A. Huertas-Vazquez, A.J. Lusis, Liver pyruvate kinase promotes NAFLD/NASH in both mice and humans in a sex-specific manner, Cell Mol. Gastroenterol. Hepatol. 11 (2021) 389–406, https://doi.org/10.1016/j.jcmgh.2020.09.004.
[10] S.L. Friedman, B.A. Neuschwander-Tetri, M. Rinella, A.J. Sanyal, Mechanisms of NAFLD development and therapeutic strategies, Nat. Med. 24 (2018) 908–922, https://doi.org/10.1038/s41591-018-0104-9.
[11] D.Q. Huang, H.B. El-Serag, R. Loomba, Global epidemiology of NAFLD-related HCC: trends, predictions, risk factors and prevention, Nat. Rev. Gastroenterol. Hepatol. 18 (2021) 223–238, https://doi.org/10.1038/s41575-020-00381-6.
[12] A. Nain-Perez, A. Foller Füchtbauer, L. Håversen, A. Lulla, C. Gao, J. Matic, L. Monjas, A. Rodríguez, P. Brear, W. Kim, M. Hyvönen, J. Borén, A. Mardinoglu, M. Uhlen, M. Grøtli, Anthraquinone derivatives as ADP-competitive inhibitors of liver pyruvate kinase, Eur. J. Med. Chem. 234 (2022), 114270, https://doi.org/10.1016/j.ejmech.2022.114270.
[13] C.J. Wenthur, P.R. Gentry, T.P. Mathews, C.W. Lindsley, Drugs for allosteric sites on receptors, Annu. Rev. Pharmacol. Toxicol. 54 (2014) 165–184, https://doi.org/10.1146/annurev-pharmtox-010611-134525.
[14] J.S. McFarlane, T.A. Ronnebaum, K.M. Meneely, A. Chilton, A.W. Fenton, A. L. Lamb, Changes in the allosteric site of human liver pyruvate kinase upon activator binding include the breakage of an intersubunit cation-π bond, Acta Crystallogr. F Struct. Biol. Commun. 75 (2019) 461–469, https://doi.org/10.1107/S2053230X19007209.
[15] M.B. Boxer, J.K. Jiang, M.G. vander Heiden, M. Shen, A.P. Skoumbourdis, N. Southall, H. Veith, W. Leister, C.P. Austin, H.W. Park, J. Inglese, L.C. Cantley, D. S. Auld, C.J. Thomas, Evaluation of substituted N,N′-diarylsulfonamides as activators of the tumor cell specific M2 isoform of pyruvate kinase, J. Med. Chem. 53 (2010) 1048–1055, https://doi.org/10.1021/jm901577g.
[16] Y. Matsui, I. Yasumatsu, T. Asahi, T. Kitamura, K. Kanai, O. Ubukata, H. Hayasaka, S. Takaishi, H. Hanzawa, S. Katakura, Discovery and structure-guided fragment-linking of 4-(2,3-dichlorobenzoyl)-1-methyl-pyrrole-2-carboxamide as a pyruvate kinase M2 activator, Bioorg. Med. Chem. 25 (2017) 3540–3546, https://doi.org/10.1016/j.bmc.2017.05.004.
[17] J. Kang Jiang, M.B. Boxer, M.G. vander Heiden, M. Shen, A.P. Skoumbourdis, N. Southall, H. Veith, W. Leister, C.P. Austin, H.W. Park, J. Inglese, L.C. Cantley, D. S. Auld, C.J. Thomas, Evaluation of thieno[3,2-b]pyrrole[3,2-d]pyridazinones as activators of the tumor cell specific M2 isoform of pyruvate kinase, Bioorg. Med. Chem. Lett. 20 (2010) 3387–3393, https://doi.org/10.1016/j.bmcl.2010.04.015.
[18] M.J. Walsh, K.R. Brimacombe, H. Veith, J.M. Bougie, T. Daniel, W. Leister, L. C. Cantley, W.J. Israelsen, M.G. vander Heiden, M. Shen, D.S. Auld, C.J. Thomas, M.B. Boxer, 2-Oxo-N-aryl-1,2,3,4-tetrahydroquinoline-6-sulfonamides as activators of the tumor cell specific M2 isoform of pyruvate kinase, Bioorg. Med. Chem. Lett. 21 (2011) 6322–6327, https://doi.org/10.1016/j.bmcl.2011.08.114.
[19] W. Yang, Z. Lu, Pyruvate kinase M2 at a glance, J. Cell Sci. 128 (2015) 1655–1660, https://doi.org/10.1242/jcs.166629.
[20] C. Kung, J. Hixon, S. Choe, K. Marks, S. Gross, E. Murphy, B. Delabarre, G. Cianchetta, S. Sethumadhavan, X. Wang, S. Yan, Y. Gao, C. Fang, W. Wei, F. Jiang, S. Wang, K. Qian, J. Saunders, E. Driggers, H.K. Woo, K. Kunii, S. Murray, H. Yang, K. Yen, W. Liu, L.C. Cantley, M.G. vander Heiden, S.M. Su, S. Jin, F. G. Salituro, L. Dang, Small molecule activation of pkm2 in cancer cells induces serine auxotrophy, Chem. Biol. 19 (2012) 1187–1198, https://doi.org/10.1016/j.chembiol.2012.07.021.
[21] Inc. Agios Pharmaceuticals, PYRUKYND® (mitapivat) approved in the EU for the treatment of pyruvate kinase (PK) deficiency in adult patients first and only disease-modifying therapy for EU patients with rare blood disorder. www.agios.com, 2022.
[22] M.A.E. Rab, B.A. van Oirschot, P.A. Kosinski, J. Hixon, K. Johnson, V. Chubukov, L. Dang, G. Pasterkamp, S. van Straaten, W.W. van Solinge, E.J. van Beers, C. Kung, R. van Wijk, AG-348 (Mitapivat), an allosteric activator of red blood cell pyruvate kinase, increases enzymatic activity, protein stability, and ATP levels over a broad range of PKLR genotypes, Haematologica 106 (2021) 238–249, https://doi.org/10.3324/haematolL.2019.238865.
[23] S. Li, H.Y. Tan, N. Wang, F. Cheung, M. Hong, Y. Feng, The potential and action mechanism of polyphenols in the treatment of liver diseases, Oxid. Med. Cell. Longev. (2018), https://doi.org/10.1155/2018/8394818, 2018.
[24] U.M. Battisti, C. Gao, F. Akladios, W. Kim, H. Yang, C. Bayram, I. Bolat, M. Kilicliogl, N. Yuksel, O.O. Tozlu, C. Zhang, J. Sebhaoui, S. Iqbal, S. Shoaie, A. Hacimuftuoglu, S. Yildirim, H. Turkez, M. Uhlen, J. Boren, A. Mardinoglu, M. Grøtli, Ellagic acid and its metabolites as potent and selective allosteric inhibitors of liver pyruvate kinase, Nutrients 15 (2023) 577, https://doi.org/10.3390/nu15030577.
[25] M.B. Boxer, J.K. Jiang, M.G. vander Heiden, M. Shen, A.P. Skoumbourdis, N. Southall, H. Veith, W. Leister, C.P. Austin, H.W. Park, J. Inglese, L.C. Cantley, D. S. Auld, C.J. Thomas, Evaluation of substituted N,N′-diarylsulfonamides as activators of the tumor cell specific M2 isoform of pyruvate kinase, J. Med. Chem. 53 (2010) 1048–1055, https://doi.org/10.1021/jm901577g.
[26] S. Liljenberg, A. Nain-Perez, O. Nilsson, J. Matic, M. Grøtli, Environmentally friendly catechol-based synthesis of dibenzosultams, New J. Chem. 46 (2022) 5593–5605, https://doi.org/10.1039/D2NJ00088A.
[27] U.L.C. Chemical Computing Group, Molecular Operating Environment (MOE), 2021, 2019.01.